universität wien

DIPLOMARBEIT

Discretized Best-Response Dynamics

for Cyclic Games

angestrebter akademischer Grad

Magister der Naturwissenschaften (Mag. rer. nat.)

Verfasser:	Peter Bednarik
Matrikel-Nummer:	0226316
Studienrichtung:	Mathematik
Betreuer:	Univ.-Prof. Dr. Josef Hofbauer

Wien, im Juli 2011

Danksagung

Allen voran möchte ich mich bei Prof. Josef Hofbauer bedanken, dessen Hilfeleistung, Verständnis und Verfügbarkeit weit über die Pflichten eines Diplomarbeitsbetreuers hinaus gingen. Ich danke meiner Frau Sonja und meinen Eltern für ihre Unterstützung, vor allem in den letzten Wochen der Fertigstellung. Des Weiteren bedanke ich mich bei Raphael Fuchs für seine Hilfe beim Programmieren, bei Prof. Viktor Avrutin für die hilfreiche Korrespondenz und bei Helene Weigang für erholsame Kaffeepausen und inspirierende Gespräche.

Contents

Abstract

The main objective of this work is to examine the behavior of the Best-Response dynamics in discrete time in the context of games known as *Hawk-Dove*, *Rock-Paper-Scissors*, or *Battle of Sexes (Odd or Even)* games. Due to its discontinuity, there are remarkable differences to the continuous-time version. In particular, we will see that by discretization, asymptotically stable fixed points can turn into repellors surrounded by an annulus shaped attracting region. In such situations we measure the inner and outer radius of the attracting region that is replacing an attracting point and investigate what happens when scaling down the discretization step, i.e. moving towards the continuous-time version. For one-dimensional systems, the outer radius turns out to diminish with the same order as the discretization step, while for two-dimensional systems it will diminish with the order of its square-root. The inner radius does not behave continuously with respect to the discretization step in the one-dimensional case and diminishes with linear order in the two-dimensional case.

In section 1, we give an overview of the theory of stable one-dimensional piecewise-linear discontinuous maps, which leads to the analysis of border-collision bifurcations. We then apply the results for Hawk-Dove games. We show a method for construction of the attractor in two-dimensional systems in section 2, where we focus on the Rock-Paper-Scissors game. In section 3, we adapt this method for a slightly different dynamics of the Rock-Paper-Scissors game as well as for the Battle of Sexes game.

Deutsche Zusammenfassung

Diese Arbeit beschäftigt sich mit dem Verhalten der Best-Response-Dynamik in diskreter Zeit in Zusammenhang mit Spielen, die als *Falken-Tauben-*, *Stein-Schere-Papier-* und *Kampf der Geschlechter-* Spiel bekannt sind. Wegen der Unstetigkeit der Best-Response Dynamik gibt es einige wesentliche Unterschiede zu ihrem zeitkontinuierlichen Pendant. Insbesondere werden wir sehen, dass sich durch die Diskretisierung asymptotisch stabile Fixpunkte in Repeller verwandeln können, welche von einem ringförmigen Attraktor umgeben sind. In solchen Fällen betrachten wir den inneren und äußeren Radius des Attraktors, der an die Stelle des stabilen Fixpunktes tritt. Wenn man die Schrittweite der Diskretisierung h gegen Null gehen lässt - und sich somit der zeitkontinuierlichen Version annähert - so verkleinert sich der äußere Radius im eindimensionalen Fall linear mit h und im zweidimensionalen Fall nur mit Ordnung von $\sqrt{h}$. Der innere Radius verhält sich im eindimensionalen Fall unstetig (bzgl. h) und linear mit h im zweidimensionalen Fall.

Kapitel 1 gibt einen Überblick über stabile eindimensionale stckweise lineare unstetige Abbildungen, wobei Border-Collision Bifurkationen eine wichtige Rolle spielen. Sodann werden die erhaltenen Resultate auf Falken-Tauben Spiele angewendet. In Kapitel 2 entwickeln wir eine Methode zur Konstruktion des Attraktors für zweidimensionale Systeme anhand des Stein-Schere-Papier Spiels. Jene wird dann in Section 3 auf eine etwas andere Dynamik, sowie auf das Kampf der Geschlechter Spiel angewendet.

1 Hawk-Dove Games

1.1 Introduction

In nature as well as in social and economic problems, we often encounter a situation where two individuals rival over a certain desirable resource. Such conflicts can occur many times repeatedly, and we are interested in their evolutionary outcome. The model will be as follows:
In a population, each turn each player can choose from two strategies, one being "aggressive"(A) and the other being "defensive" (D). Depending on their and on the other player's choice, both players get a payoff, corresponding to the expected success in exploiting the desirable resource. A very prominent setting for this situation was given by John Maynard Smith in [7], where (A) corresponds to "hawkish" and (D) to "dovish" behavior, which is where the name *Hawk-Dove Game* comes from.
If player I is aggressive and player II cautious, we assume that player I will get the entire resource V while player II gets nothing. If both players are cautious, they either share the resource or one of them (randomly!) retreats earlier and the other gets the entire resource. In any case the expected outcome is that they both get half of it ($V/2$). Finally, if both players are aggressive, there will be a fight resulting in severe injuries C for the loser. As before, we assume that the winner is determined randomly, and that both players suffer an expected loss $(V-C)/2$. The only interesting case is when the risk of injury is larger than value of the resource, thus we will always assume that $C > V$. We can summarize the payoffs Π (being gains of the resource as well as losses in form of injuries) for each player in a *payoff-matrix*:

$$\begin{pmatrix} \frac{V-C}{2} & V \\ 0 & \frac{V}{2} \end{pmatrix} \tag{1.1}$$

From our assumptions it is immediately clear, that if one player knew the other player's choice, the only rational reply would be to use the opposite strategy. In other words, players will try to discoordinate on their strategies, which explains why this type of interactions is sometimes also called "anti-coordination" games. In the past, these games have been studied under different circumstances, the most prominent among them being the *Hawk-Dove Game* [7] as mentioned above, the *Chicken Game* or the *Snowdrift Game*.
Imagine a population of players, where each turn they are put into random pairs to play the game. Which strategy should a player use? For this purpose let us denote the fraction of aggressive (A) players by $x \in [0, 1]$. Thus, according to the payoff-matrix (1.1), if a player chooses to play (A), (s)he gets the payoff

$$\Pi(A) = x\frac{V-C}{2} + (1-x)V$$

and if a player chooses (C), (s)he gets

$$\Pi(D) = (1-x)\frac{V}{2}$$

A player should use (A) whenever $\Pi(A) > \Pi(D)$ and vice versa.

$$\begin{aligned}
\Pi(A) > \Pi(D) \quad &\Leftrightarrow \quad x\frac{V-C}{2} + (1-x)V > (1-x)\frac{V}{2} \\
&\Leftrightarrow \quad x\frac{V-C}{2} + (1-x)\frac{V}{2} > 0 \\
&\Leftrightarrow \quad x\frac{-C}{2} + \frac{V}{2} > 0 \\
&\Leftrightarrow \quad x < \frac{V}{C}
\end{aligned}$$

Next part of our model is that we assume that after each turn, a fraction ϵ of the players update their strategy in order to maximize their payoffs.

$$x' = f(x) = \begin{cases} f_L(x) = (1-\epsilon)x + \epsilon & \text{if } x < q \\ f_R(x) = (1-\epsilon)x & \text{if } x > q \end{cases} \tag{1.2}$$

with $q = \frac{V}{C}$. In the following we want to analyze this dynamics in dependence of the parameters ϵ and q, $\epsilon < 1$, $0 < q < 1$. We will see that this seemingly simple system permits quite complex behavior including periodic orbits of any arbitrary period. First, we can shift the dynamical system towards the origin to obtain

$$x' = f(x) = \begin{cases} f_L(x) = (1-\epsilon)x + \epsilon(1-q) & \text{if } x < 0 \\ f_R(x) = (1-\epsilon)x - \epsilon q & \text{if } x > 0 \end{cases} \tag{1.3}$$

Now, we can apply an elegant method introduced by N.N. Leonov in the late 1950's. Before that, let us remark that if we let $\epsilon \to 0$ we get the well-understood continuous-time Best-Response dynamics instead of dynamics (1.2)

$$\dot{x} = \begin{cases} 1-x & \text{if } x < q \\ -x & \text{if } x > q \end{cases} \tag{1.4}$$

Obviously, for (1.4), the equilibrium q is globally asymptotically stable.

1.2 Leonov's approach

The following argument is due to Leonov (1959)[5], which was almost forgotten and discovered but in the recent years [4]. In this section, I give only a short summary of the main idea. The next section will provide pictures and less abstract applications. A detailed description of the general method is given in [5] and [4]. In order to use it, we need to consider a slightly more general situation:

$$x' = f(x) = \begin{cases} f_L(x) = \lambda_L x + a & \text{if } x < 0 \\ f_R(x) = \lambda_R x - b & \text{if } x > 0 \end{cases} \tag{1.5}$$

with $a, b > 0$, $\lambda_L < 1$ and $\lambda_R < 1$. Since there can be no fixed points, we seek to find out about possible periodic orbits. If such exist, they must be asymptotically stable because any composition of f_L and f_R is a contraction due to $\lambda_L \lambda_R < 1$. Obviously, if $x < 0$, then $f(x) < a$ and if $x > 0$, then $f(x) > -b$ which means that it is impossible to leave the interval

$$I = [-b, a] \tag{1.6}$$

On the other hand, if $x < 0$ then $x' > x$ and if $x > 0$ then $x' < x$, which means that all orbits must end up in I. Hence, we will consider only points $x \in I$ from now on.
In this context, it is often convenient to use a symbolic notation: We count the times of an orbit being on the left (L) or on the right (R) side of the discontinuity point and thus get symbolic sequences of the form e.g. $LRLRR$, corresponding to $(f_R \circ f_R \circ f_L \circ f_R \circ f_L)(x)$.
First, let us see why symbolic sequences of the form $L^m R^n$ do not exist for $m, n > 1$. Assume there were such a sequence, then we get a contradiction by

$$\begin{aligned} m > 1, n > 1 \quad &\Rightarrow \quad f(-b) < 0, \quad f(a) > 0 \\ &\Rightarrow \quad a < \lambda_L b, \quad b < \lambda_R a \\ &\Rightarrow \quad a < \lambda_L \lambda_R a \end{aligned} \tag{1.7}$$

Following Leonov [5], and Gardini et al.[4], we divide periodic orbits in different classes. Those periodic orbits having exactly one point in one region, and $n \geq 1$ points on the other regions (i.e. $x = (f_R^n \circ f_L)(x)$ or $x = (f_R \circ f_L^n)(x)$, respectively), we will say to be of *first level of complexity* (cf. Figure 1.1).

For existence of the orbit corresponding to LR^n we need to have $f_L(-b) > 0$. We seek to find a map g, which maps the interval $(-b, 0)$ into itself. Clearly, there must exist n, such that $(f_R^n \circ f_L)(-b) \in (-b, 0)$. Now we have to consider two cases: Either also the other end of our interval fulfills $(f_R^n \circ f_L)(0) \in (-b, 0)$, or $(f_R^n \circ f_L)(0) > 0$.
In the first case,

$$g = f_R^n \circ f_L \tag{1.8}$$

is a contracting map $(-b, 0) \mapsto (-b, 0)$ and therefore has a unique fixed point. In the

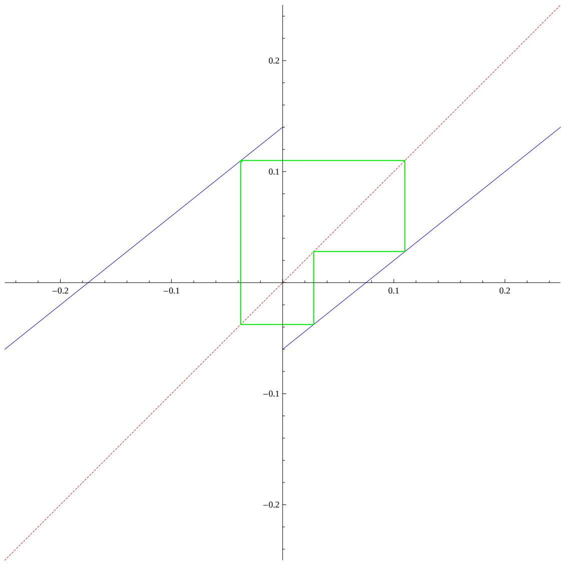

(a) Periodic orbit of first level of complexity with parameters $\lambda_L = \lambda_R = 0.8$, $a = 0.14$, $b = 0.06$ ($\epsilon = 0.2$, $q = 0.3$)

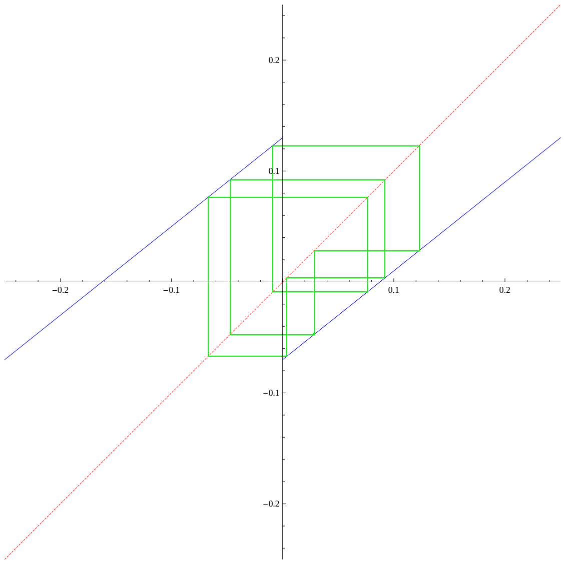

(b) Periodic orbit of second level of complexity with parameters $\lambda_L = \lambda_R = 0.8$, $a = 0.13$, $b = 0.07$ ($\epsilon = 0.2$, $q = 0.35$)

Figure 1.1: Typical periodic orbits of first and second level of complexity, respectively.

latter case we note that $(f_R^{(n+1)} \circ f_L)(0) \in (-b, 0)$, because

$$\begin{aligned}
\lambda_L \lambda_R < 1 \quad &\Rightarrow \quad a - \lambda_R a > \lambda_L b - b \\
&\Rightarrow \quad a - \lambda_L b > \lambda_R a - b \\
&\Rightarrow \quad f_L(-b) > f_R(f_L(0)) \\
&\Rightarrow \quad (f_R^{n+1} \circ f_L)(0) < (f_R^n \circ f_L)(-b)
\end{aligned}$$

Thus, in the case $(f_R^n \circ f_L)(0) > 0$, we can define

$$g(x) = \begin{cases} g_L(x) = (f_R^n \circ f_L)(x) & \text{if } (f_R^n \circ f_L)(x) < 0 \\ g_R(x) = (f_R^{n+1} \circ f_L)(x) & \text{if } (f_R^n \circ f_L)(x) > 0 \end{cases} \tag{1.9}$$

which is a discontinuous map from $(-b, 0)$ to itself, very much like the one we have started with, which is the main observation for the upcoming iterative reasoning.
Since f is piecewise linear, it is easy to compute arbitrary powers of the map. In particular, we are interested in $f_R^n \circ f_L$:

$$\begin{aligned}
x' &= f_L(x) = \lambda_L x + a \\
x'' &= f_R(x') = \lambda_R(\lambda_L x + a) - b \\
x''' &= f_R(x'') = \lambda_R(\lambda_R(\lambda_L x + a) - b) - b \\
&\vdots \\
x^{(n+1)} &= \lambda_R^n(\lambda_L x + a) - b(1 + \lambda_R + \lambda_R^2 + \ldots + \lambda_R^{n-1}) \\
&= \lambda_R^n(\lambda_L x + a) - b\frac{1 - \lambda_R^n}{1 - \lambda_R} \qquad (1.10) \\
&= (f_R^n \circ f_L)(x)
\end{aligned}$$

which has the fixed point

$$\hat{x} = \frac{1}{1 - \lambda_L \lambda_R^n} \left(a\lambda_R^n - b\frac{1 - \lambda_R^n}{1 - \lambda_R} \right) \tag{1.11}$$

Obviously, the two inequalities

$$-b \leq \hat{x} = (f_R^n \circ f_L)(\hat{x}) \leq 0 \tag{1.12}$$

are necessary and sufficient for existence of the fixed point. In other words, (1.12) gives a region of parameters, where a periodic orbit of complexity level one exists. If it does not exist, we can perform a change of variables towards the origin. By using (1.9) and (1.10) we get

$$y = x - (f_R^n \circ f_L)^{-1}(0) = x - \frac{b\frac{1-\lambda^n}{1-\lambda} - a\lambda^n}{\lambda^{n+1}} \tag{1.13}$$

$$g(y) = \begin{cases} g_L(y) = \tilde{\lambda} y + \tilde{a} & \text{if } y < 0 \\ g_R(y) = \tilde{\lambda} y - \tilde{b} & \text{if } y > 0 \end{cases} \tag{1.14}$$

with

$$\begin{aligned}
\tilde{\lambda}_L &= \lambda_L \lambda_R^n \\
\tilde{\lambda}_R &= \lambda_L \lambda_R^{n+1} \\
\tilde{a} &= \frac{a}{\lambda_L} - \frac{b}{\lambda_L} \frac{1-\lambda_R^n}{1-\lambda_R} \\
\tilde{b} &= \frac{a}{\lambda_L} - b\left(1 + \frac{1}{\lambda_L} \frac{1-\lambda_R^n}{1-\lambda_R}\right)
\end{aligned}$$

Thus, we can make use of our previous calculation and we define the periodic orbits of *of complexity level two* for map f as periodic orbits of complexity level one for map g. So far, we assumed that $f(-b) > 0$ and hence analyzed $f_R^n \circ f_L$. Of course, they symmetric case $f(a) < 0$ leads to analogous results when considering $f_L^n \circ f_R$. Thus, periodic orbits of second level of complexity are fixed points of either $LR^n(LR^{n+1})^m, LR^{n+1}(LR^n)^m$, $RL^n(RL^{n+1})^m$, or $RL^{n+1}(RL^n)^m$. Their parameter regions of existence are given by

$$-\tilde{b} \leq \hat{y} \leq 0 \tag{1.15}$$

where $\hat{y}$ is the fixed point for the appropriate map. As one can imagine we obtain periodic orbits of higher complexity levels by iterating the above reasoning. Furthermore, in principal it is possible to calculate all bifurcation curves analytically by using this method.

Of course, there are many more things to say about this procedure (among them being that it ends in finitely many steps for the whole parameter region minus a set of zero measure [4]), however those are beyond the scope of this work and we will continue by applying the above theory to anti-coordination games.

1.3 Application to Hawk-Dove Games

We return to

$$x' = f(x) = \begin{cases} f_L(x) = (1-\epsilon)x + \epsilon & \text{if } x < q \\ f_R(x) = (1-\epsilon)x & \text{if } x > q \end{cases} \tag{1.16}$$

with $\epsilon < 1$, and $0 < q < 1$ from (1.2) and hence we have two parameters less than in the previous chapter. Comparing (1.3) with (1.5) we get

$$a = \epsilon(1-q) \qquad b = \epsilon q \tag{1.17}$$

Thus, by undoing the shift of the origin, the attracting interval from (1.6) turns to

$$I = [q - \epsilon q, q + \epsilon(1-q)] \tag{1.18}$$

Further, we can see that

$$\begin{aligned} q \le \frac{1}{2} \quad &\Rightarrow \quad q < \frac{1}{2-\epsilon} \\ &\Rightarrow \quad q(\epsilon^2 - 2\epsilon) > -\epsilon \\ &\Rightarrow \quad q((1-\epsilon)^2 - 1) > -\epsilon \\ &\Rightarrow \quad q(1-\epsilon)^2 + \epsilon = f(q - \epsilon q) > q \end{aligned} \tag{1.19}$$

and

$$\begin{aligned} q \ge \frac{1}{2} \quad &\Rightarrow \quad q > \frac{1-\epsilon}{2-\epsilon} \\ &\Rightarrow \quad q < \frac{\epsilon^2 - \epsilon}{\epsilon^2 - 2\epsilon} \\ &\Rightarrow \quad q(\epsilon^2 - 2\epsilon) + \epsilon - \epsilon^2 < 0 \\ &\Rightarrow \quad (1-\epsilon)(q + \epsilon(1-q)) = f(q + \epsilon(1-q)) < q \end{aligned} \tag{1.20}$$

Due to the argument in (1.7) and below, if $q \le \frac{1}{2}$, the orbits can stay at the left side of the equilibrium q at most once in succession. If $q \ge \frac{1}{2}$, the orbits can stay at the right side of the equilibrium q at most once in succession. It follows that for the symmetric case $q = \frac{1}{2}$ there can be only a periodic orbit of period 2. It is the solution of $f_R(f_L(x)) = x$ which is globally asymptotically stable and is given by

$$\hat{x} = \frac{1-\epsilon}{2-\epsilon}, \quad f_L(\hat{x}) = \frac{1}{2-\epsilon} \tag{1.21}$$

Due to symmetry, it is sufficient to focus on the case $q < \frac{1}{2}$ from now on. Here, periodic orbits of first level of complexity are of the form LR^n. With the abbreviation $\lambda = 1 - \epsilon$ we have

$$f_R^{(n)}(f_L(x)) = \lambda^{n+1}x + \lambda^n - \lambda^{n+1} \tag{1.22}$$

which has the fixed point

$$\hat{x} = \frac{\lambda^n \epsilon}{1 - \lambda^{n+1}} \tag{1.23}$$

For each $n \geq 1$, equation (1.23) gives the smallest point of the periodic orbit (with period $n+1$) of first level of complexity. The regions of existence of these orbits are given by (1.12) and the corresponding bifurcation[1] curves can be obtained by solving $\hat{x} = q$, and $\hat{x} = q - \epsilon q$, respectively.

$$q_L^{LR^n} = \frac{(1-\epsilon^n)\epsilon}{1-(1-\epsilon)^{n+1}} \tag{1.24}$$

$$q_R^{LR^n} = \frac{(1-\epsilon^n)\epsilon}{1-(1-\epsilon)^{n+2}-\epsilon} \tag{1.25}$$

According to the previous chapter, we get the periodic orbits of second level of complexity by replacing the map f by $f_L^n \circ f_R$ or $f_L \circ f_R^n$. Thus we get the four families of bifurcation curves for periodic orbits of second level of complexity (with $\lambda = 1 - \epsilon$):

$$q_L^{LR^n(LR^{n+1})^m} = \frac{\left(-1+\left(\lambda^{2+n}\right)^{1+m}\right)\lambda^n\epsilon}{\left(-1+\lambda^{2+n}\right)\left(1+\lambda^n\left(\lambda^{2+n}\right)^m(-\lambda)\right)} \tag{1.26}$$

$$q_R^{LR^n(LR^{n+1})^m} = -\frac{\lambda^{n-1}\epsilon\left(\lambda+\left(\lambda^{2+n}\right)^m\left(-\lambda^{2+n}+\epsilon\right)\right)}{\left(-1+\lambda^{2+n}\right)\left(1+\lambda^n\left(\lambda^{2+n}\right)^m(-\lambda)\right)} \tag{1.27}$$

$$q_L^{LR^{n+1}(LR^n)^m} = \frac{\left(-1+\left(\lambda^{1+n}\right)^{1+m}\right)\lambda^n\epsilon}{-1+\lambda^n+\lambda^n\left(\left(1-\lambda^{1+n}\right)\left(\lambda^{1+n}\right)^m\lambda^2-\epsilon\right)} \tag{1.28}$$

$$q_R^{LR^{n+1}(LR^n)^m} = \frac{\lambda^n\epsilon\left(-1+\left(\lambda^{1+n}\right)^m\left(\lambda^{2+n}+\epsilon\right)\right)}{-1+\lambda^n+\lambda^n\left(\left(1-\lambda^{1+n}\right)\left(\lambda^{1+n}\right)^m\lambda^2-\epsilon\right)} \tag{1.29}$$

A detailed calculation is given in [4]. All together, we can put the analytically calculated bifurcation curves into a picture (Figure 1.2). Note that for $q \geq 1/2$ we get the same picture as Figure 1.2 mirrored along the $q = 1/2$ axis. In between of any regions in Figure 1.2 are infinitely many other regions. However, as stated in the previous chapter, not all of the area is covered since a set of zero measure remains and is not corresponding to any periodic orbit.

[1]These are so-called Border-collision bifurcations, as first mentioned in [6]

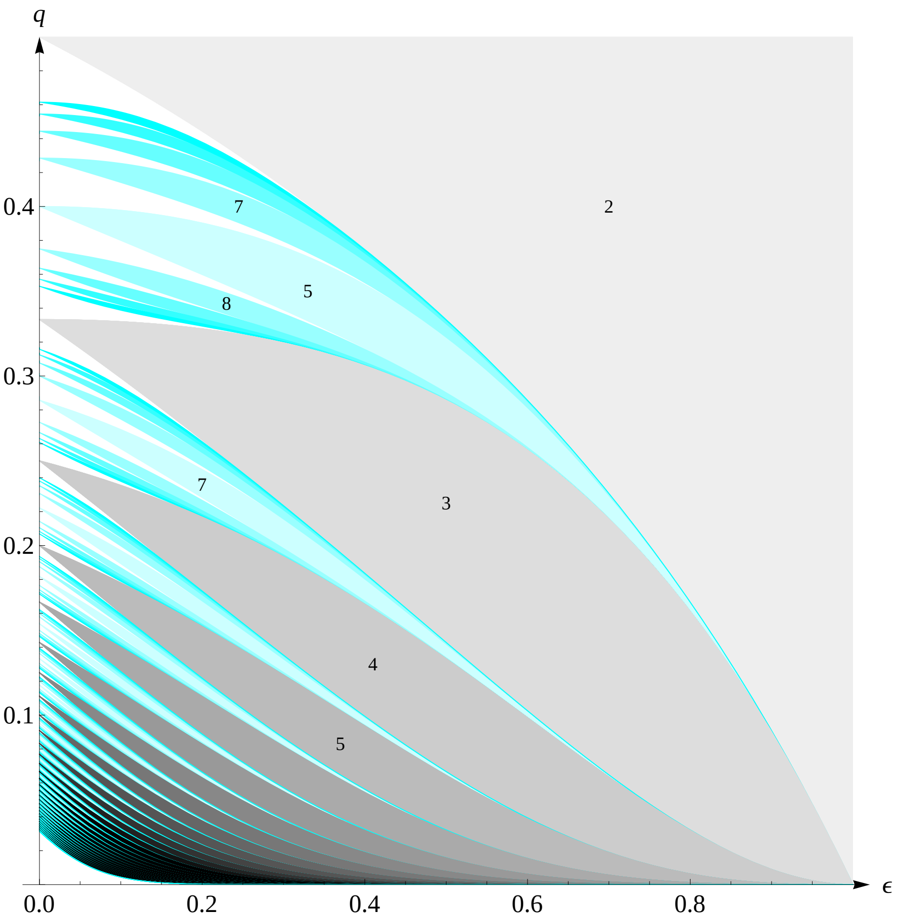

Figure 1.2: Bifurcation Curves of periodic orbits of first level of complexity (gray color, up to $n = 30$) and second order of complexity (blue color, up to $m = 5$) calculated analytically. The numbers are indicating the period of periodic orbits in the corresponding regions. While the orbits of first level of complexity are all of the form LR^k, there are different types of second level complexity orbits. For the examples in the figure these are: the upper 7-cycle has the form $LR^2(LR)^2$, the 5-cycle $LRLR^2$, the 8-cycle $LR(LRR)^2$ and the lower 7-cycle LR^2LR^3

In order to even better understand what happens, let us look at the example where $q = 0.35$ (Figure 1.3), which simply means taking out a line from Figure 1.2. We can see clearly that with smaller and smaller ϵ, new periodic orbits always emerge on the boundary of the attracting interval $[q - \epsilon q, q + \epsilon(1 - q)]$.

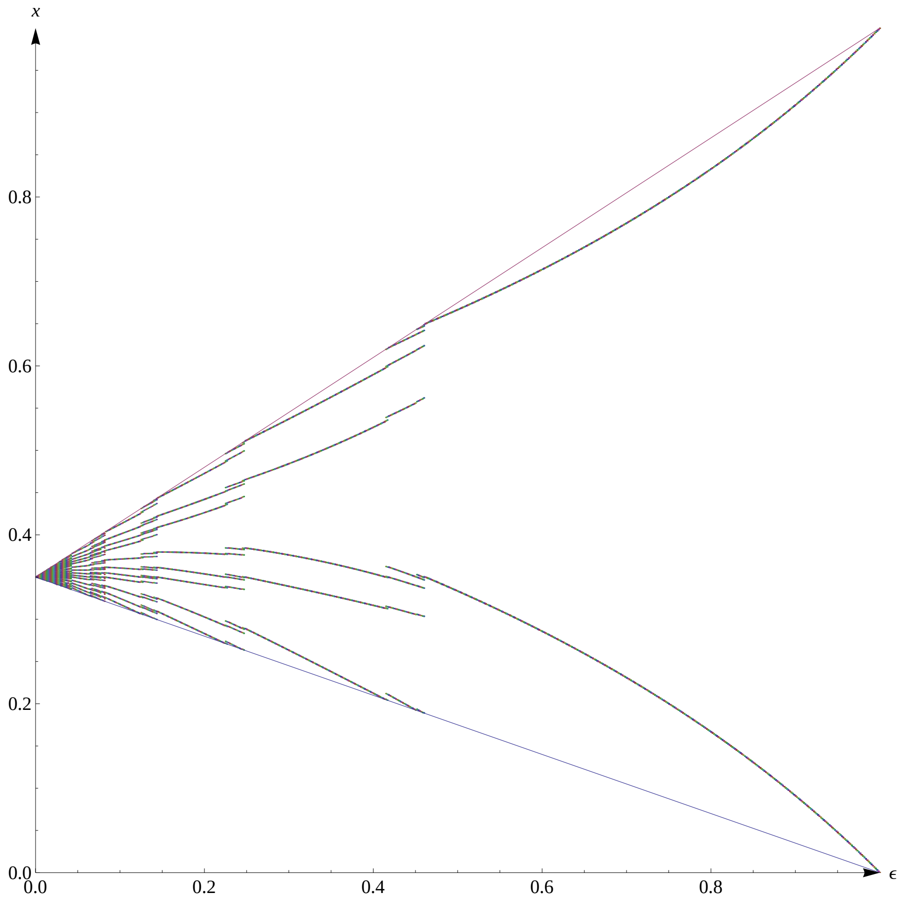

Figure 1.3: Numerical calculation of the bifurcation diagram for $q = 0.35$. Observe that for (approximately) $\epsilon > 0.46$ the attractor is a 2-cycle(LR). For $0.25 < \epsilon < 0.41$ it is a 5-cycle($LRLRR$), for $0.14 < \epsilon < 0.22$ it is an 8-cycle($LR(LRR)^2$) and so forth.

As a final remark let us again consider the periodic orbits of first level of complexity:

$$\hat{x} = \frac{\lambda^n \epsilon}{1 - \lambda^{n+1}} \tag{1.30}$$

The sum of all points of this periodic orbit is given by

$$\begin{aligned}
\sum_{k=0}^{n} f_R^{(k)}(f_L(\hat{x})) &= \sum_{k=0}^{n} \lambda^k(\lambda\hat{x} + 1 - \lambda) \\
&= (\lambda\hat{x} + 1 - \lambda)\frac{1 - \lambda^{n+1}}{1 - \lambda} \\
&= 1 - \lambda^{n+1} + \lambda\hat{x}\frac{1 - \lambda^{n+1}}{1 - \lambda} \\
&= \lambda\frac{\lambda^n(1 - \lambda)}{1 - \lambda^{n+1}} \cdot \frac{1 - \lambda^{n+1}}{1 - \lambda} + 1 - \lambda^{n+1} \\
&= 1
\end{aligned} \tag{1.31}$$

And thus the time average $\bar{x}$ of the periodic orbit with period n is given by

$$\bar{x} = \frac{1}{n} \tag{1.32}$$

This is remarkable because it is independent of ϵ and q, as long as the periodic orbit of the given period exists. Numerical tests also indicate that a more general result holds: If l denotes the number of points of the periodic orbit on the left side of q and n is its period, then

$$\bar{x} = \frac{l}{n} \tag{1.33}$$

However, I did not yet succeed in proving this conjecture for periodic orbits of complexity larger than one.

2 Rock-Paper-Scissors Games

2.1 Introduction

Now, we move on to two-dimensional systems. In this section we will analyze a discretization of the Best-Response dynamics for rock-paper-scissor games. For $x \in \Delta_3 \subset \mathbb{R}^3$ consider

$$x' = F(x) = (1-\epsilon)x + \epsilon \mathrm{BR}(x) \tag{2.1}$$

or, with $\epsilon = \frac{h}{1+h}$

$$x' = F(x) = \frac{1}{1+h}(x + h\mathrm{BR}(x)) \tag{2.2}$$

where $\mathrm{BR}(x)$ is the best response to the current state x, more precisely, following Hofbauer [2], we define

$$\mathrm{BR}(x) := \underset{y\in\Delta}{\operatorname{argmax}}(yAx) = \left\{ y \in \Delta : yAx = \max_{z\in\Delta}(zAx) \right\} \tag{2.3}$$

for the payoff matrix

$$A = \begin{pmatrix} 0 & -1 & 1 \\ 1 & 0 & -1 \\ -1 & 1 & 0 \end{pmatrix}$$

In general, $\mathrm{BR}(x)$ is a set, however we will focus on the case where it consists of a single point. Then

$$\mathrm{BR}(x) = \begin{cases} p_2 = (0,1,0), & \text{if } x \in A_1 := \{x \in \Delta_3 : x_1 > 1/3 \wedge x_3 < 1/3\} \\ p_3 = (0,0,1), & \text{if } x \in A_2 := \{x \in \Delta_3 : x_2 > 1/3 \wedge x_1 < 1/3\} \\ p_1 = (1,0,0), & \text{if } x \in A_3 := \{x \in \Delta_3 : x_3 > 1/3 \wedge x_2 < 1/3\} \end{cases} \tag{2.4}$$

For the continuous-time Best-Response dynamics we recall that the equilibrium is globally asymptotically stable [3]. However, in our case, will see that the situation is quite different. We have

$$F(x) = \begin{cases} F_1(x) = \frac{1}{1+h}(x_1, x_2 + h, x_3), & \text{if } x \in A_1 \\ F_2(x) = \frac{1}{1+h}(x_1, x_2, x_3 + h), & \text{if } x \in A_2 \\ F_3(x) = \frac{1}{1+h}(x_1 + h, x_2, x_3), & \text{if } x \in A_3 \end{cases} \tag{2.5}$$

We are primarily interested in the behavior on A_1, A_2, and A_3. The lines $l_1 = \{(x_1, x_2, x_3) \in \Delta_3 : x_1 = 1/3, x_3 < 1/3\}$, $l_2 = \{(x_1, x_2, x_3) \in \Delta_3 : x_2 = 1/3, x_1 < 1/3\}$ and $l_3 = \{(x_1, x_2, x_3) \in \Delta_3 : x_3 = 1/3, x_2 < 1/3\}$ in between of those regions can be seen as limiting cases of either of the two adjacent regions, as we will see in the following arguments (cf. Figure 2.1).

2.2 Construction of an Attractor

Now we want to give good estimates for the global attractor of the system. We will show that it is a region topologically equivalent to a ring.

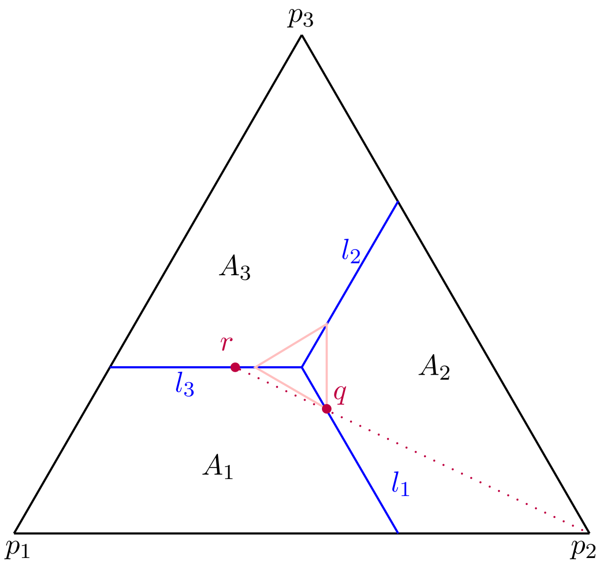

Figure 2.1: Constructing a repelling neighborhood of the center

Let us consider the point $q = (q_1, q_2, q_3)$ on the line l_1, such that its pre-image $F_1^{-1}(q) = r = (r_1, r_2, r_3)$ is on the line l_3. We will show that the points inside the equilateral triangle produced by the corners q, Tq and T^2q do not possess a pre-image, where T is the rotation $T(x_1, x_2, x_3) = (x_2, x_3, x_1)$. First, let us compute this point in dependence of the parameter h.
We have that $F_1(r) = \frac{1}{1+h}(r_1, r_2 + h, r_3)$. From $r_3 = \frac{1}{3}$ we get $q_3 = \frac{1}{3} \cdot \frac{1}{1+h}$, and with $q_1 = \frac{1}{3}$ we get

$$q_2 = 1 - q_1 - q_3 = 1 - \frac{1}{3} - \frac{1}{3} \cdot \frac{1}{1+h} = \frac{1}{3} \cdot \frac{1+2h}{1+h}$$

All together:

$$q = \frac{1}{3}\left(1, \frac{1+2h}{1+h}, \frac{1}{1+h}\right) \tag{2.6}$$

The line from q to Tq is given by $x_1 = x_3 + \frac{1}{3} \cdot \frac{h}{1+h}$. Now we can show that the points $x' = (x'_1, x'_2, x'_3)$ in A_1 with $x'_1 < x'_3 + \frac{1}{3} \cdot \frac{1}{1+h}$ do not have any pre-image $x = (x_1, x_2, x_3)$.

Proof. It is clear that x' cannot have a pre-image in A_2. Let us assume that x' has a pre-image $x \in A_1$. Then we get a contradiction by

$$\frac{1}{3} < x'_1 < x'_3 + \frac{1}{3} \cdot \frac{h}{1+h} = \frac{1}{1+h}\left(x_3 + \frac{h}{3}\right) < \frac{1}{1+h}\left(\frac{1}{3} + \frac{h}{3}\right) < \frac{1}{3} \tag{2.7}$$

Finally, to check that also a pre-image in A_3 is impossible, we first calculate

$$
\begin{aligned}
x_1' &< x_3' + \frac{1}{3}\cdot\frac{h}{1+h} < \frac{1}{3}\left(1+\frac{h}{1+h}\right) = \frac{1}{3}\cdot\frac{1+2h}{1+h} \\
\Longrightarrow \qquad 0 &< -x_1'(1+h) + \frac{1}{3}(1+2h) \\
\Longrightarrow \qquad \frac{1}{3}(1+h) &< \frac{1}{3}(1+h) + \frac{1}{3}(1+2h) - x_1'(1+h) \\
&< \frac{2}{3} + h - x_1'(1+h)
\end{aligned}
\tag{2.8}
$$

Now, assuming $x \in A_3$, we get

$$
x_3 = x_3'(1+h) < \frac{1}{3}(1+h) < \frac{2}{3} + h - x_1'(1+h) = \frac{2}{3} - x_1 \tag{2.9}
$$

However, in A_3 the sum $x_1 + x_3$ must be $> \frac{2}{3}$, completing the proof. $\square$

Now, let us try to find an estimation for ω-limits of the orbits. Following orbits from A_1 we see that not all points of A_2 can be reached. The image $F_1(l_1)$ is a line parallel to l_1, because of $F_1(x_1, x_2, x_3) = \frac{1}{1+h}(x_1, x_2 + h, x_3)$ meaning that the first coordinate is constant. From the strip between l_1 and $F_1(l_1)$ the orbits move towards l_2. So, by tracking the point $q_0 = (\frac{1}{3}, \frac{2}{3}, 0)$ we see the border between the points in A_2 that may be reached from A_1 and the points in A_2 that are inaccessible from A_1. Note that the orbit of $(\frac{1}{3}, \frac{2}{3}, 0)$ meets the line l_2 in Δ_3°.

We want to construct a mapping $G : l_1 \to l_1$, such that all orbits under the dynamics F of points in A_1 are inside of the orbit of q_0 under G. The idea is already in the above paragraph: We take $F(q_0)$ and connect to the line l_2. Then, we can use symmetry to interpret the result as a point on l_1. More precisely, let

$$
G = T \circ Z \circ F \tag{2.10}
$$

where T is the rotation and $Z : A_2 \to l_2$ the projection onto l_2 in direction of p_3. So, we have

$$
T(x_1, x_2, x_3) = (x_2, x_3, x_1) \tag{2.11}
$$

To get Z, let us denote $Z(x_1, x_2, x_3)$ by $(\tilde{x}_1, \tilde{x}_2, \tilde{x}_3)$. Applying the Intercept Theorem (see Fig. 2.3) we get

$$
\frac{x_1}{\tilde{x}_1} = \frac{1 - x_3}{1 - \tilde{x}_3} \tag{2.12}
$$

Since $Zx \in l_2$ we also have

$$
\tilde{x}_1 + \tilde{x}_3 = \frac{2}{3} \tag{2.13}
$$

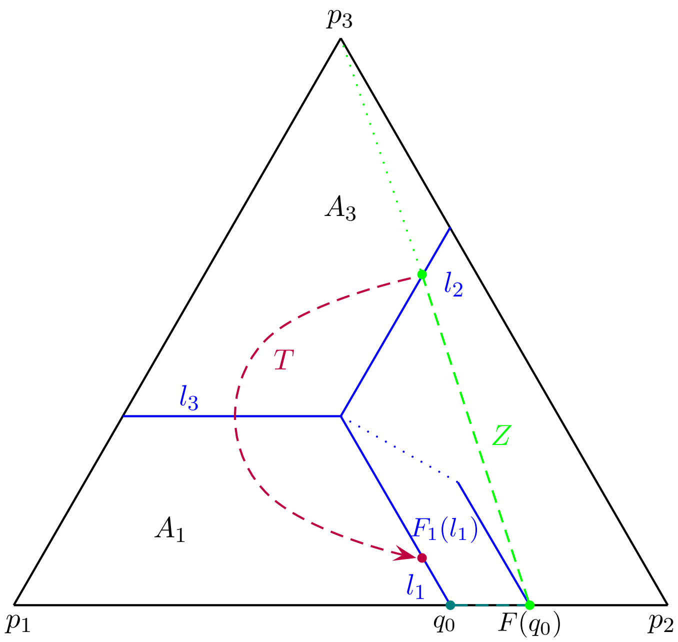

Figure 2.2: Constructing an Attracting Region

And thus we can write

$$\begin{aligned}
\tilde{x}_1 &= \frac{x_1}{1-x_3}\left(1-\frac{2}{3}+\tilde{x}_1\right) \\
\implies \qquad \tilde{x}_1\left(1-\frac{x_1}{1-x_3}\right) &= \frac{x_1}{1-x_3}\cdot\frac{1}{3} \\
\implies \qquad \tilde{x}_1 &= \frac{1}{3}\cdot\frac{x_1}{1-x_3}\Big/\left(1-\frac{x_1}{1-x_3}\right) \\
&= \frac{1}{3}\cdot\frac{x_1}{1-x_3}\cdot\frac{1-x_3}{1-x_1-x_3} \\
&= \frac{x_1}{3x_2}
\end{aligned}$$

All together, we get

$$Z\begin{pmatrix} x_1 \\ x_2 \\ x_3 \end{pmatrix} = \frac{1}{3}\begin{pmatrix} \frac{x_1}{x_2} \\ 1 \\ 2-\frac{x_1}{x_2} \end{pmatrix} \tag{2.14}$$

and by (2.10):

$$\begin{aligned}
G : l_1 &\to l_1 \\
\frac{1}{3}\begin{pmatrix} 1 \\ 3x_2 \\ 2-3x_1 \end{pmatrix} &\mapsto \frac{1}{3}\begin{pmatrix} 1 \\ 2-\frac{1}{3}\frac{1}{x_2+h} \\ \frac{1}{3}\frac{1}{x_2+h} \end{pmatrix}
\end{aligned} \tag{2.15}$$

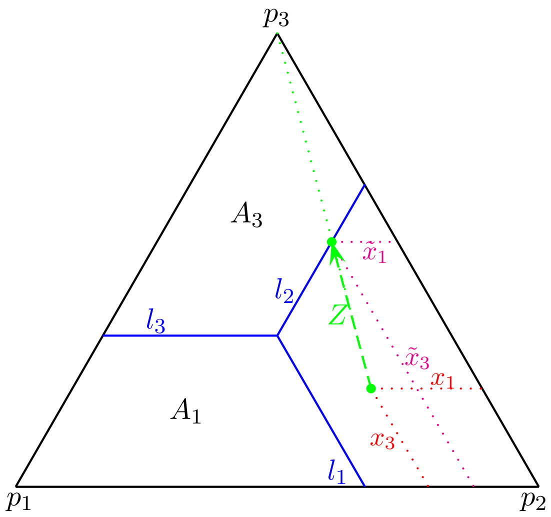

Figure 2.3: Using the Intercept Theorem to get Z

Since l_1 is a line, it suffices to consider one coordinate

$$g: \; x_2 \mapsto \frac{1}{9}\left(6 - \frac{1}{x_2 + h}\right) \tag{2.16}$$

Because $g'(x) = \frac{1}{9} \cdot \frac{1}{(x_2+h)^2} < 1$, g is contracting and therefore also G is contracting, which means that there exists a unique stable fixed point $\hat{x}$. It is immediately clear that $\hat{x} \neq q_0$ and also that $\hat{x}$ is not the equilibrium (because it is a repeller). Thus, the orbit of $\hat{x}$ under G is an outer boundary for all orbits of A_1 (and thus for all points in Δ_3) under the original dynamics F.
To get $\hat{x}$, we simply solve

$$9x_2 = 6 - \frac{1}{x_2 + h} \tag{2.17}$$

and obtain

$$\hat{x}_2 = \frac{1}{6}\left(2 - 3h + \sqrt{3h}\sqrt{3h+4}\right) \tag{2.18}$$

and hence

$$\hat{x} = \frac{1}{6}\begin{pmatrix} 2 \\ 2 - 3h + \sqrt{3h}\sqrt{3h+4} \\ 2 + 3h - \sqrt{3h}\sqrt{3h+4} \end{pmatrix} = \frac{1}{3}\begin{pmatrix} 1 \\ 1 \\ 1 \end{pmatrix} + \frac{1}{6}\begin{pmatrix} 0 \\ -3h + \sqrt{3h}\sqrt{3h+4} \\ 3h - \sqrt{3h}\sqrt{3h+4} \end{pmatrix} \tag{2.19}$$

2.3 Periodic Orbits

Let us try to find analytic expressions for periodic orbits of (2.2). The first step is to calculate $F^n(x)$ for $x \in A_1$:

$$\begin{aligned}
F(x) = x' &= \frac{1}{1+h}\begin{pmatrix} x_1 \\ x_2 + h \\ x_3 \end{pmatrix} \\
F(F(x)) = x'' &= \frac{1}{(1+h)^2}\begin{pmatrix} x_1 \\ x_2 + h + h(1+h) \\ x_3 \end{pmatrix} \\
F^{(n)}(x) &= \frac{1}{(1+h)^n}\begin{pmatrix} x_1 \\ x_2 + h\frac{1-(1+h)^n}{1-(1+h)} \\ x_3 \end{pmatrix} \\
&= \frac{1}{(1+h)^n}\begin{pmatrix} x_1 \\ x_2 + (1+h)^n - 1 \\ x_3 \end{pmatrix} \qquad (2.20)
\end{aligned}$$

If $\hat{x}_n$ is a periodic orbit of period $3n$, then

$$T(\hat{x}_n) = F^{(n)}(\hat{x}_n) \tag{2.21}$$

with rotation T as above. Solving this linear equation gives

$$\hat{x}_n = \frac{1}{1+(1+h)^n+(1+h)^{2n}}\begin{pmatrix} (1+h)^{2n} \\ 1 \\ (1+h)^n \end{pmatrix} \tag{2.22}$$

From

$$\frac{(1+h)^n}{1+(1+h)^n+(1+h)^{2n}} = \frac{(1+h)^n}{((1+h)^n-1)^2+3(1+h)^n} < \frac{1}{3}$$

and

$$\frac{(1+h)^{2n}}{1+(1+h)^n+(1+h)^{2n}} > \frac{1}{3}$$

it follows that for all $n \geq 1$

$$\hat{x}_n \in A_1 \tag{2.23}$$

or, equivalently, $F^{(n)}(\hat{x}_n) \in A_2$. Thus, a periodic orbit of period 3 must exist for all $h \geq 0$ and periodic orbits of period $3n$ exist for h, such that

$$F^{n-1}(\hat{x}_n) = \frac{1}{1+(1+h)^n+(1+h)^{2n}}\begin{pmatrix} (1+h)^{n+1} \\ (1+h)^{2n} - h(1+(1+h)^n) \\ 1+h \end{pmatrix} \in A_1 \tag{2.24}$$

which is equivalent to

$$\frac{(1+h)^{n+1}}{1+(1+h)^n+(1+h)^{2n}} \geq \frac{1}{3} \tag{2.25}$$

As expected, if $n = 1$, this condition holds for all $h > 0$, and for $n \geq 2$ there is a threshold h_n, such that inequality (2.25) holds for $h < h_n$. In other words, as h gets smaller, higher period orbits emerge, while the lower periodic orbits will be maintained, resulting in multiple coexisting periodic orbits (cf. Figure 2.4). We can measure their distance from the center by comparing their position on the line l_1. Intersecting l_1 with the line

$$tp_2 + (1-t)\hat{x}_n \qquad\qquad t \in [0,1] \tag{2.26}$$

gives

$$\frac{1}{3}\left(2 - \frac{1}{\frac{\frac{1}{(1+h)^n}}{\frac{1}{(1+h)^n}}}\right) \tag{2.27}$$

Note that for $n = 1$ we get precisely the point q from (2.6). In Figure 2.4 we compare the x_2 coordinates of various periodic orbits.

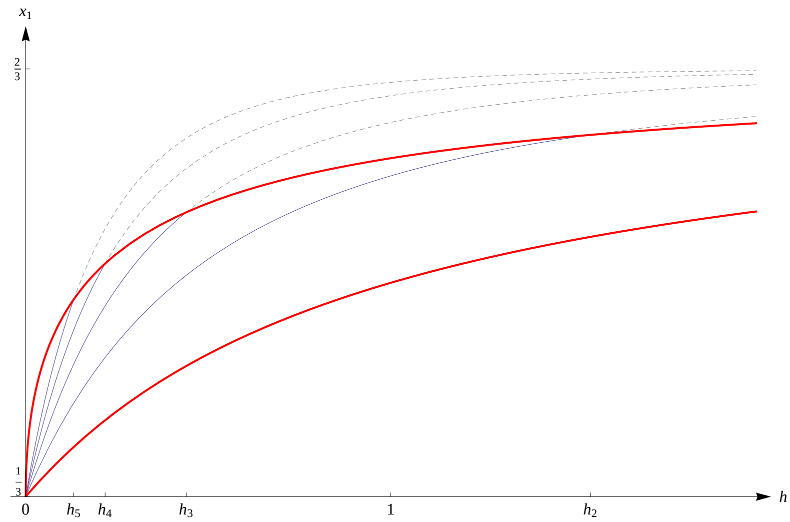

Figure 2.4: Periodic Orbits of periods $3n$, which exist for $h < h_n$, for n up to 5. The red lines correspond to the boundary of the attractor calculated in the previous section and h_k are numerical solutions to the equation corresponding to (2.25). Note the connection to Figure 2.6.

For stability of the periodic orbits, we have from (2.20) that

$$F_1^{(n)}(x_1,x_2,x_3) = \frac{1}{(1+h)^n}\begin{pmatrix} x_1 \\ x_2+(1+h)^n-1 \\ x_3 \end{pmatrix} \tag{2.28}$$

Then, we can obtain $F_2^{(n)}$ and $F_3^{(n)}$ in the same way and put them all together

$$\begin{aligned} F^{(3n)} &= F_3^{(n)}(F_2^{(n)}(F_1^{(n)}(x_1,x_2,x_3))) \\ &= \frac{1}{(1+h)^{3n}}\begin{pmatrix} x_1 \\ x_2 \\ x_3 \end{pmatrix} + \begin{pmatrix} 1-(1+h)^{-n} \\ (1+h)^{-3n}((1+h)^n-1) \\ (1+h)^{-3n}(1+h)^n((1+h)^n-1) \end{pmatrix} \end{aligned}$$

Thus, the eigenvalues of $F^{(3n)}$ are $\frac{1}{(1+h)^{3n}} < 1$ and hence all periodic orbits are stable.

2.4 Conclusion

In summary we have shown that all trajectories end up in a region bounded by the two triangles as can be seen in Figure 2.5. As h approaches 0, more and more higher period orbits emerge. Note that by construction of map G for the outer boundary, new periodic

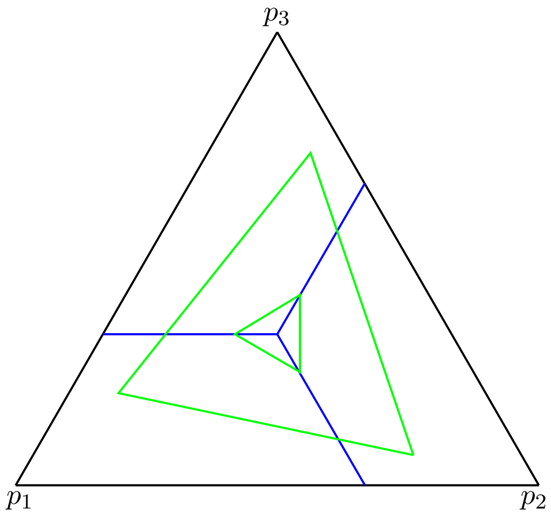

Figure 2.5: The region bounded by the two green triangles is globally attracting

orbits emerge precisely on this boundary. In other words, whenever a new periodic orbit is born, G can be seen as a Poincare-map of F, $F^{(i)}(x) = G(x)$, for some $i \in \mathbb{N}$, and $x \in l_1$. This also means that convergence of the outer boundary of the attractor towards the center cannot be faster than with order of square root in the following sense:
We can measure their distance from the center by the x_2-coordinate of their intersection with the line l_1. Then we get from (2.6) and (2.18)

$$q_2 = \frac{1}{3}\frac{1+2h}{1+h} = \frac{1}{3}\left(1+\frac{h}{1+h}\right) \overset{h\to 0}{\approx} \frac{1}{3}(1+h) \tag{2.29}$$

$$\hat{x}_2 = \frac{1}{6}\left(2-3h+\sqrt{9h^2+12h}\right) \overset{h\to 0}{\approx} \frac{1}{3}\left(1+\sqrt{3h}\right) \tag{2.30}$$

As $h \to 0$, the inner boundary converges to the center with linear order, while the outer boundary converges to the center only with order of the square-root of step size h.

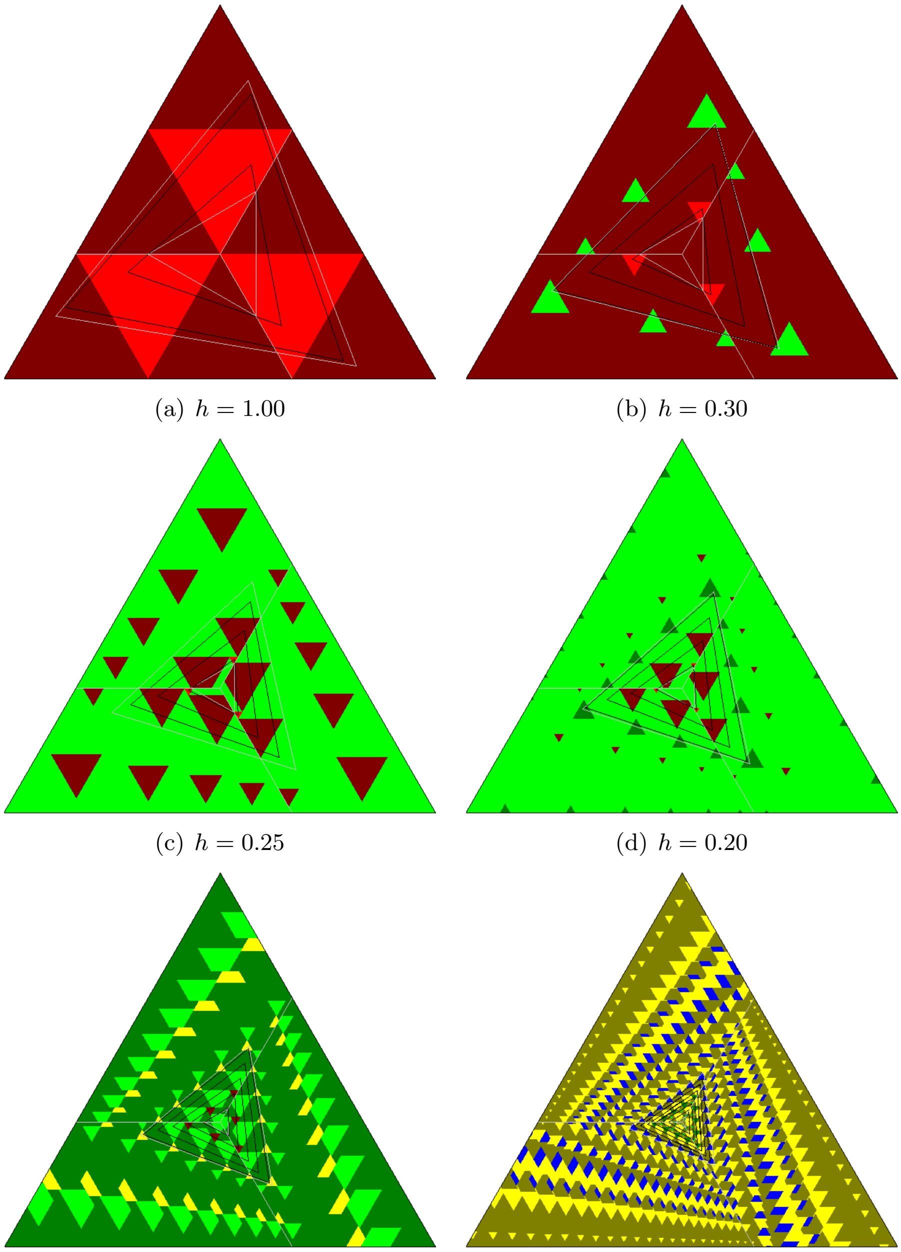

(a) $h = 1.00$ (b) $h = 0.30$

(c) $h = 0.25$ (d) $h = 0.20$

(e) $h = 0.12$ (f) $h = 0.05$

Figure 2.6: Periodic orbits of various periods together with their (numerically calculated) respective basins of attraction. Red is the basin of attraction for period 3, dark red for period 6, light green 9, and so on. The calculated boundaries of the attractor are also included (gray lines).

3 Generalization and Further Applications

3.1 A Different Dynamics

3.1.1 Continuous-time Dynamics

In this section we want to have look at a different dynamical system with piecewise linear solutions. First let us recall from [2] that in its continuous counterpart, the Brown-von Neumann-Nash dynamics, the inner equilibrium is asymptotically stable. Consider

$$\dot{x}_i \quad = \quad f(k_i) - x_i \sum_{j=1}^{n} f(k_j) \tag{3.1}$$

with

$$k_i = \begin{cases} (Ax)_i - xAx & \text{, if } (Ax)_i - xAx > 0 \\ 0 & \text{, if } (Ax)_i - xAx \leq 0 \end{cases} \tag{3.2}$$

where $f : \mathbb{R} \to \mathbb{R}$ is an integrable function such that $f(x) = 0$, for $x \leq 0$, and $f(x) > 0$ for $x > 0$, and for A, we require

$$\xi A \xi \leq 0, \text{ for } \xi \in \mathbb{R}^n, \text{ s.t.} \sum \xi_i = 0 \text{ and } \xi \neq 0 \tag{3.3}$$

which is a generalization of the the zero-sum games case.

Theorem 3.1 (Hofbauer, 2000)**.** *For games with* (3.3)*, the set of equilibria is globally asymptotically stable for* (3.1)*.*

Proof. For the antiderivative F of f, i.e. $F' = f$, let us consider

$$V(x) = \sum_i F(k_i(x)) \tag{3.4}$$

Clearly, if $k_i(x) = 0$ for all i, which is the case where x is an equilibrium, then $\dot{V}(x) = 0$. Otherwise, with the abbreviations $\bar{f} = \sum_i f(k_i)$ and $f(k) = (f(k_1), f(k_2), \ldots, f(k_n))$ and $\tilde{f} = f/\bar{f}$, we have

$$\begin{aligned} \dot{k}_i &= e_i A\dot{x} - \dot{x}Ax - xA\dot{x} \\ &= e_i A f(k) - e_i \bar{f} Ax - f(k)Ax + \bar{f}xAx - xAf(k) + xAx\bar{f} \\ &= \bar{f}\left[(e_i - x)A(\tilde{f} - x) - (\tilde{f} - x)Ax\right] \end{aligned}$$

It follows that

$$
\begin{aligned}
\dot{V} &= \sum_i F'(k_i)\dot{k_i} = \sum_i f(k_i)\dot{k_i} = \bar{f}\sum \tilde{f}_i\dot{k_i} \\
&= \bar{f}\sum_i \Big[f(k_i)e_iA\tilde{f} - f(k_i)e_iAx - f(k_i)xA\tilde{f} + \\
&\quad +f(k_i)xAx - f(k_i)\tilde{f}Ax + f(k_i)xAx\Big] \\
&= \bar{f}\left[f(k)A\tilde{f} - f(k)Ax - \bar{f}xA\tilde{f} + \bar{f}xAx - \bar{f}\tilde{f}Ax + \bar{f}xAx\right] \\
&= \bar{f}^2\left[\tilde{f}A\tilde{f} - \tilde{f}Ax - xA\tilde{f} + xAx - \tilde{f}Ax + xAx\right] \\
&= \bar{f}^2\left[(\tilde{f}-x)A(\tilde{f}-x) - (\tilde{f}-x)Ax\right] \\
&= \dot{x}A\dot{x} - \bar{f}\dot{x}Ax \qquad (3.5)
\end{aligned}
$$

which is negative. Condition (3.3) guarantees $\dot{x}A\dot{x} \le 0$ and for the second term, we have

$$
\begin{aligned}
\dot{x}Ax &= \sum_i f(k_i)(Ax)_i - \bar{f}xAx \\
&= \sum_i f(k_i)\left[(Ax)_i - xAx\right] \\
&= \sum_i f(k_i)k_i \ge 0 \qquad (3.6)
\end{aligned}
$$

□

3.1.2 Discrete-time Dynamics

Now, let us look at

$$
x_i' = \frac{x_i + hf(u_i)}{1 + h\sum_{j=1}^{3} f(u_j)} \qquad (3.7)
$$

with

$$
\begin{aligned}
h &> 0 \\
i &= 1, \ldots, 3 \\
u_i &= (Ax)_i \ \text{ with } \ x \in \Delta_3 \\
f(u_i) &= \begin{cases} 1 & \text{for } u_i > 0 \\ 0 & \text{for } u_i \le 0 \end{cases} \\
A &= \begin{pmatrix} 0 & -1 & 1 \\ 1 & 0 & -1 \\ -1 & 1 & 0 \end{pmatrix}
\end{aligned}
$$

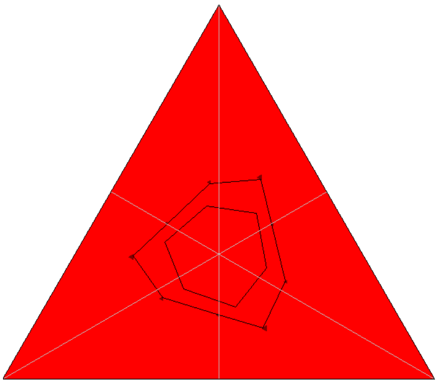

(a) $h = 0.26$

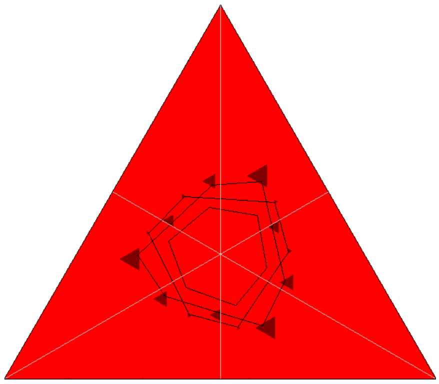

(b) $h = 0.25$

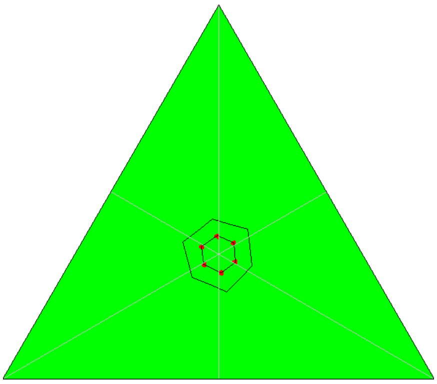

(c) $h = 0.08$

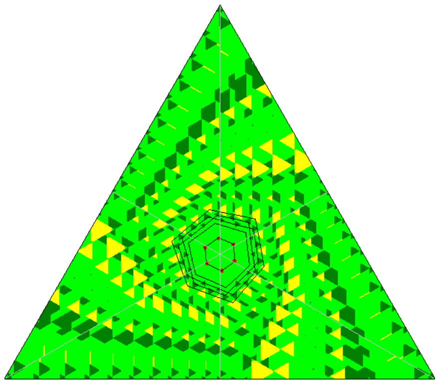

(d) $h = 0.07$

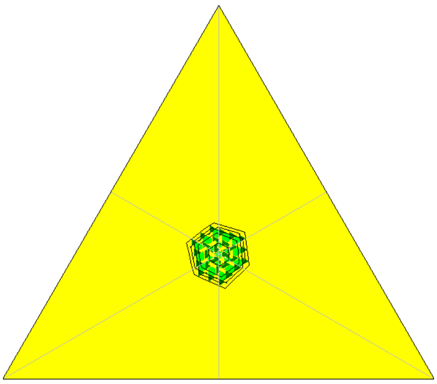

(e) $h = 0.043$

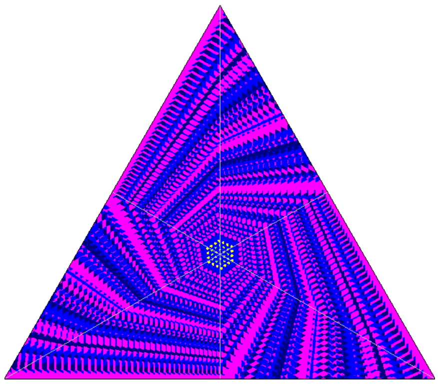

(f) $h = 0.019$

Figure 3.1: Periodic orbits of various periods together with their (numerically calculated) respective basins of attraction. Red is the basin of attraction for period 6, dark red for period 9, light green 12, dark green 15, yellow 18 and so on.

As opposed to the system in section 2, we now have to distinguish between 6 different regions instead of 3. Let us look at the region $x_3 < x_2 < x_1$. There, trajectories point towards the corner $(0, 1, 0)$. On the other hand, in region $x_3 < x_1 < x_2$, trajectories point towards $\left(0, \frac{1}{2}, \frac{1}{2}\right)$. Due to symmetry, we obtain the other 4 cases by rotation. From the reasoning in the last section, it is clear that we could proceed in the same manner to obtain the inner and outer boundaries of the attractor. However, because not all of the regions are now equivalent, this is more tedious and hence we will omit the analytic investigation and have a look at the numerical results instead.
The main difference to the situation from section 2 is that different types of periodic orbits are possible. Apart from the periodic orbits of period $6n$, $n \geq 1$, which correspond to the periodic orbits of period $3n$ from section 2, there are periodic orbits of periods $6n + 3$, $n \geq 1$. We can clearly see the two different period 9 orbits in Figure 3.1 (a) and (b). However, unlike the "symmetric" orbits (those of period $6n$), the "less symmetric" orbits of periods $6n + 3$ are not maintained when scaling down the step size h. We can see in Figure 3.1 (c) that both period 9 orbits fail to exist for $h = 0.08$ where we have only the two symmetric periodic orbits of periods 6 and 12.

To sum it up, we can see that, despite the differences in the periodic orbits, the situation is very similar to section 2. Indeed, numerical results show that also here the attracting region is annulus-shaped and its inner radius diminishes with order of h while the outer radius diminishes with order $\sqrt{h}$ of the step size as $h \to 0$.

3.2 Cyclic 2×2 Bimatrix Games

3.2.1 Introduction

Now let us consider a cyclic bimatrix game (often referred to as *Battle of Sexes*, e.g. in [1]). Due to the complexity of discontinuous discrete-time systems we will restrict our analytical analysis to the symmetric case, however we will give numerical simulations of asymmetric cases at the end of this section. Now, the game is played by two players or populations, which adjust their strategies every turn. 2×2 means that they have both two strategies to choose from where also *mixed* strategies are allowed: When interpreting the players as individuals, we say that players can choose *probabilities*, i.e. to play strategy 1 with probability x and strategy 2 with probability $1-x$. When interpreting the players as populations, we say that the populations are large numbers of individuals each playing a pure strategy. Then, we can assign the *proportions* x and $1-x$ to individuals of one population to play strategy 1 or strategy 2, respectively. Thus, the *payoff* for player 1 and player 2, respectively is given by

$$\Pi^1 = (x, 1-x)A(y, 1-y)^T \tag{3.8}$$
$$\Pi^2 = (y, 1-y)B(x, 1-x)^T \tag{3.9}$$

where A and B are 2×2 payoff matrices, and x and y are real numbers in $[0,1]$. As before, we use the discrete-time Best-Response dynamics, which means that every turn, a fraction of each population changes their strategy according to the best response of the last round. It is easy to see that player 1's best response is either $x=1$, if

$$e_1 A(y, 1-y)^T > e_2 A(y, 1-y)^T \tag{3.10}$$

or $x=0$, otherwise. Similarly, player 2's best response is either $y=1$, if

$$e_1 B(x, 1-x)^T > e_2 B(x, 1-x)^T \tag{3.11}$$

or $y=0$, otherwise.

3.2.2 Symmetric Case

For the analytical analysis we will use a simplified case, where

$$A = -B^T = \begin{pmatrix} 1 & -1 \\ -1 & 1 \end{pmatrix} \tag{3.12}$$

and where in each turn, a fraction $\frac{h}{1+h}$ changes to the best response. All together, this yields the following dynamics

$$(x', y') = F(x,y) = \frac{1}{1+h} \cdot \begin{cases} (x, y) & \text{if } x > \frac{1}{2}, y < \frac{1}{2} \\ (x, y+h) & \text{if } x < \frac{1}{2}, y < \frac{1}{2} \\ (x+h, y+h) & \text{if } x < \frac{1}{2}, y > \frac{1}{2} \\ (x+h, y) & \text{if } x > \frac{1}{2}, y > \frac{1}{2} \end{cases} \tag{3.13}$$

which gives four regions of $[0,1]\times[0,1]$, in each of which the orbits point towards the respective corners.

First, let us calculate the periodic orbit having exactly one point in each of the four

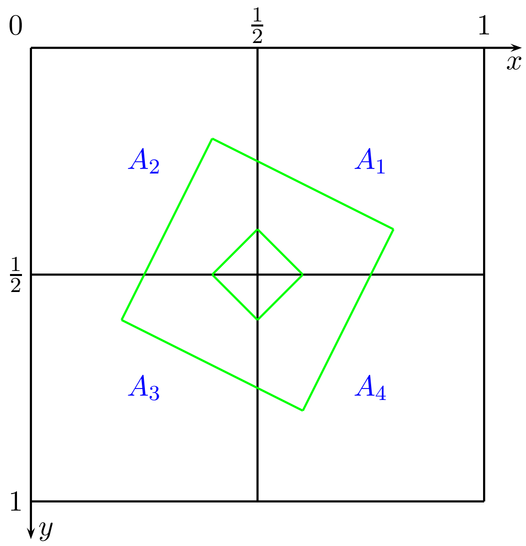

Figure 3.2: All trajectories end up in the region bounded by the green squares.

regions. We arbitrarily choose region A_1, and thus for $x > 1/2, y < 1/2$, we have to solve the linear equation

$$\begin{pmatrix} x \\ y \end{pmatrix} = TF \begin{pmatrix} x \\ y \end{pmatrix} = \frac{1}{1+h} \begin{pmatrix} 1-y+h \\ x \end{pmatrix} \tag{3.14}$$

where $T(x,y) := (1-y,x)$ is the clockwise orthogonal rotation. Its solution

$$\begin{pmatrix} x \\ y \end{pmatrix} = \frac{1}{1+(1+h)^2} \begin{pmatrix} (1+h)^2 \\ 1+h \end{pmatrix} \tag{3.15}$$

is satisfying $x > 1/2$ and $y < 1/2$ for all $h > 0$ which means that it also exists for all $h > 0$. Like in the Rock-Paper-Scissor game from the previous section, we could also calculate periodic orbits of any period $4n$, $n \geq 1$. A straightforward calculation in the same fashion as before shows, that also in this setting, the higher period cycles exist for certain thresholds $h < h_n$.

Now we proceed with showing that the intersection of the lines between points of the period 4 cycle (3.15) with the axes also gives a boundary of the attractor of (3.13). Those intersections are given by

$$q = \frac{1}{2}\left(1, 1 - \frac{h}{1+h}\right) \tag{3.16}$$

and its rotations. The line in A_1 connecting these points is given by $x = y + \frac{1}{2}\cdot\frac{h}{1+h}$ (small green square in Figure 3.2).

Proposition 3.2. *The points in A_1 with $x < y + \frac{1}{2} \cdot \frac{h}{1+h}$ do not have a pre-image under F.*

Proof. Clearly, the region under consideration cannot have a pre-image in A_2 or A_3. Let $(x, y) \in A_1$. Then

$$x < y + \frac{1}{2}\frac{h}{1+h} < \frac{1}{2} + \frac{1}{2}\frac{h}{1+h} = \frac{1}{2}\frac{1+2h}{1+h} \tag{3.17}$$

and therefore

$$x' < \frac{1}{2}\frac{1+2h}{(1+h)^2} < \frac{1}{2} \tag{3.18}$$

and thus $(x', y') \notin A_1$. Now, if $(x, y) \in A_4$, then, assuming the contrary,

$$x' < y' + \frac{1}{2} \cdot \frac{h}{1+h} < \frac{1}{2}\frac{1+2h}{1+h} \tag{3.19}$$

and hence

$$x = x'(1+h) - h < \frac{1}{2}(1+2h) - h = \frac{1}{2} \tag{3.20}$$

gives a contradiction to $(x, y) \in A_4$. □

Next, we want to compute the outer boundary of the attractor of (3.13). Let us consider orbits of points in region A_1 and let us denote the lines $l_1 = \{(x, y) : x = \frac{1}{2}, 0 \leq y \leq \frac{1}{2}\}$ and $l_2 = \{(x, y) : y = \frac{1}{2}, 0 \leq x \leq \frac{1}{2}\}$. No matter where we start, most of region A_2 cannot be reached by those orbits, namely the points left of the line $F(l_1) = \{(x, y) \in A_2 : x < \frac{1}{2}\frac{1}{1+h}\}$. Which part of A_3 can be reached from here?
Of course, again the furthest we can get is $F(l_2)$ but we also see that all points must be on the right hand side of the point given by projecting $(\frac{1}{2}, 0)$ onto l_2 in direction of $(0, 1)$. This central (perspective) projection is given by

$$Z(x, y) = \frac{1}{2}\left(\frac{x}{1-y}, 1\right) \tag{3.21}$$

Further, due to symmetry of the dynamical system, we can identify l_2 with l_1 simply by rotating 90° in clockwise direction, which is represented by the mapping $T(x, y) := (1-y, x)$. Clearly, we get a mapping $G : l_1 \to l_1$ with $G = T \circ Z \circ F$. Explicitly, we have

$$G(1/2, y) = \frac{1}{2}\left(1, \frac{1}{2-2y+2h}\right) \tag{3.22}$$

which has a unique fixed point $(1/2, \hat{y})$, which is a solution of

$$y = g(y) = \frac{1}{2-2y+2h} \tag{3.23}$$

Together with $y < 1/2$ we get that

$$\hat{y} = \frac{1}{2}\left(1 + h - \sqrt{2h + h^2}\right) \tag{3.24}$$

Because $g' = \frac{dg}{dy} = \frac{1}{\left(1+h+\sqrt{h(2+h)}\right)^2} < 1$, we know that $\hat{y}$ is asymptotically stable under the map g and thus $(1/2, \hat{y})$ is asymptotically stable under G.
What we have achieved, is that all orbits under F must be inside of the orbit of $(1/2, \hat{y})$ under G. In other words, the orbit of $(1/2, \hat{y})$ under G is an outer boundary for the attractor of F. It is worth noting that when making h smaller and smaller, new periodic orbits emerge exactly when $G(1/2, \hat{y}) = F^k(1/2, \hat{y})$ for some $k \in \mathbb{N}$. From equations (3.16) and (3.24) we get similar estimates as in (2.29):

$$q_y = \frac{1}{2}\left(1 - \frac{h}{1+h}\right) \overset{h\to 0}{\approx} \frac{1}{2}(1-h) \tag{3.25}$$

$$\hat{y} = \frac{1}{2}\left(1 + h - \sqrt{2h + h^2}\right) \overset{h\to 0}{\approx} \frac{1}{2}\left(1 - \sqrt{2h}\right) \tag{3.26}$$

Thus, we have the same result as in section 2.4, namely that as $h \to 0$, the inner boundary converges to the center with linear order of step size h, while the outer boundary converges to the center only with order of the square-root.

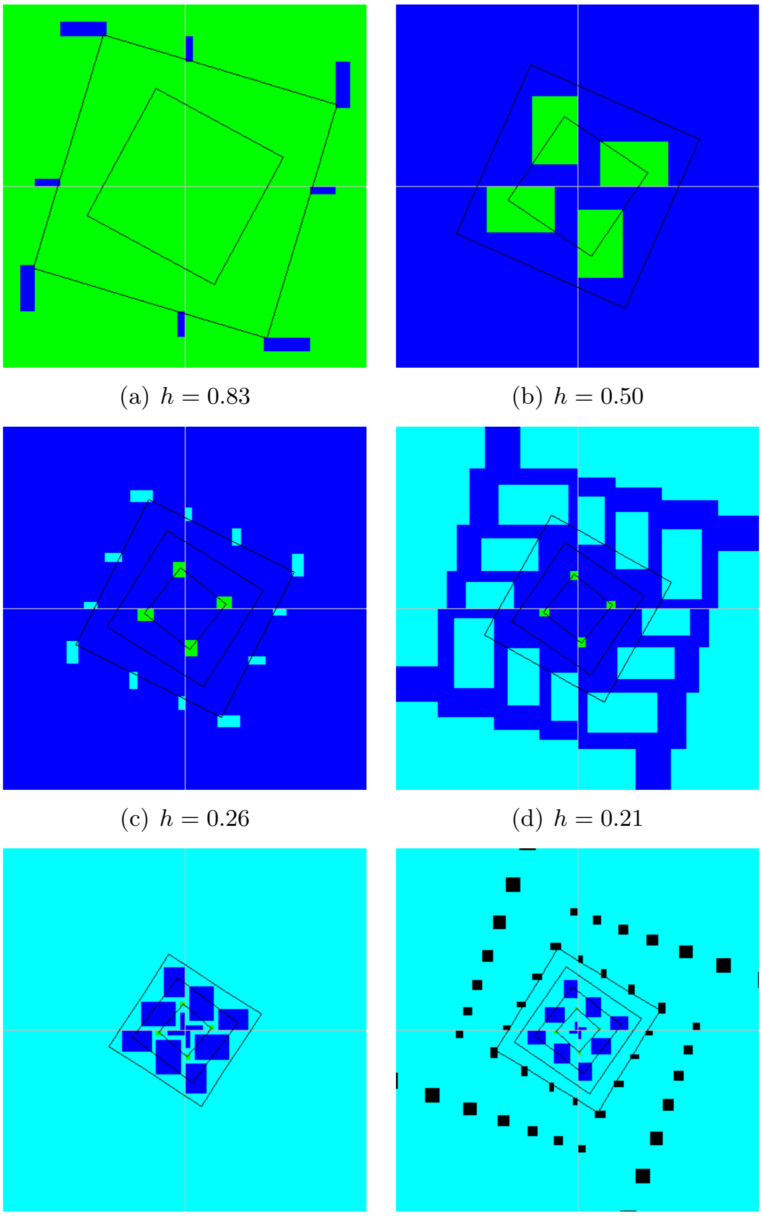

(a) $h = 0.83$ (b) $h = 0.50$

(c) $h = 0.26$ (d) $h = 0.21$

(e) $h = 0.16$ (f) $h = 0.13$

Figure 3.3: Periodic orbits of various periods together with their (numerically calculated) respective basins of attraction. Green is the basin of attraction for period 4, blue for period 8, teal 12, and so on.

3.2.3 Continuous-time Dynamics

Let us have a brief look what happens if we let $h \to 0$ and thus consider the continuous-time version of dynamics (3.13). If $y < 1/2$, then

$$\begin{aligned} x' &= \frac{x}{1+h} \quad \text{, or} \\ \frac{x'-x}{h} &= x' \end{aligned}$$

and with $h \to 0$

$$\dot{x} = -x$$

If, on the other hand, $y > 1/2$, then

$$\begin{aligned} x' &= \frac{x}{1+h} \quad \text{, or} \\ \frac{x'-x}{h} &= 1-x' \end{aligned}$$

and with $h \to 0$

$$\dot{x} = 1-x$$

With similar results for y we get the continuous-time Best-Response dynamics for the game (3.12)

$$\begin{aligned} \dot{x} &= b^1 - x \\ \dot{y} &= b^2 - x \end{aligned} \tag{3.27}$$

where (b^1, b^2) is a corner of $[0,1]^2$. Now let us consider

$$V(x,y) := |x - 1/2| + |y - 1/2| \tag{3.28}$$

Then we can see that $\dot{V} = -V$, because:
If $x \geq 1/2$ and $y \leq 1/2$, then $V = x - y \Rightarrow \dot{V} = \dot{x} - \dot{y} = -x + y = -V$.
If $x \geq 1/2$ and $y \geq 1/2$, then $V = x + y - 1 \Rightarrow \dot{V} = \dot{x} + \dot{y} = 1 - x - y = -V$.
If $x \leq 1/2$ and $y \leq 1/2$, then $V = 1 - x - y \Rightarrow \dot{V} = -\dot{x} - \dot{y} = x - (1 - y) = -V$.
If $x \leq 1/2$ and $y \geq 1/2$, then $V = -x + y \Rightarrow \dot{V} = -\dot{x} + \dot{y} = -(1 - x) + (1 - y) = -V$.
Thus,

$$V(t) = V(0)e^{-t} \to 0 \tag{3.29}$$

which means that the distance to the equilibrium $(1/2, 1/2)$ is decreasing exponentially. In particular, it is asymptotically stable, unlike in the discrete-time version.

3.2.4 Examples of Asymmetric 2D Systems

So far, we have investigated symmetric two-dimensional systems. In the first section we analyzed asymmetric one-dimensional systems via Leonov's method. In that case no multiple steps within one of the two regions were possible and there were no coexisting orbits. Instead, asymmetry of the system caused the existence of asymmetric periodic orbits of various complexities. It is beyond the scope of this work to construct a theory for two dimensions based on Leonov's approach, however an example shall indicate that this should be possible. Proceeding as in sections 3.2.1 and 3.2.2, but using the matrix

$$A = -B^T = \begin{pmatrix} 1 & -2 \\ -1 & 1 \end{pmatrix} \tag{3.30}$$

and $h = 0.09$ gives the following picture. According to the numerical calculation, there

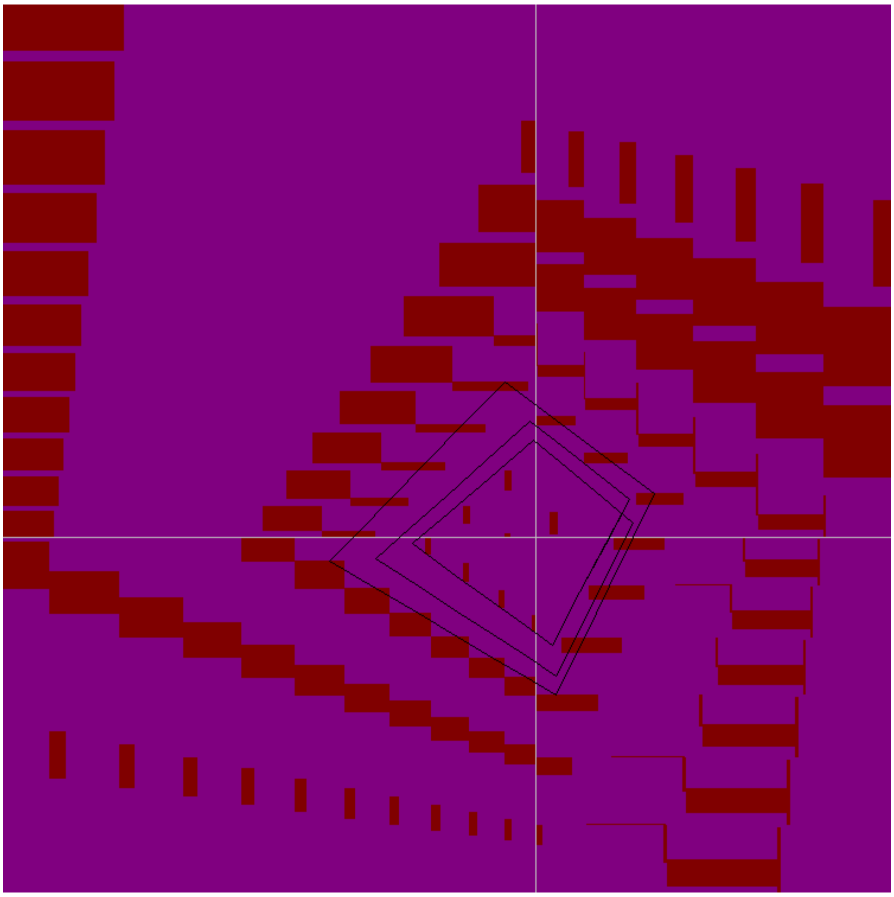

Figure 3.4: Asymmetric 2D System

are two periodic orbits. The outer one has period 18 and is "simple" while the inner has period 26 and is what we should call *of second level of complexity* in two dimensions.

4 Appendix

4.1 Mathematica Code of Figures

4.1.1 Figure 1.2

```
Plots = Table[
   Plot[{((1 - \[Epsilon])^n \[Epsilon])/(
     1 - (1 - \[Epsilon])^(
      1 + n)), -(((1 - \[Epsilon])^
       n \[Epsilon])/(-1 + (1 - \[Epsilon])^(
       2 + n) + \[Epsilon])), ((-1 + ((1 - \[Epsilon])^(2 + n))^(
        1 + m)) (1 - \[Epsilon])^
      n \[Epsilon])/((-1 + (1 - \[Epsilon])^(
        2 + n)) (1 + (1 - \[Epsilon])^n ((1 - \[Epsilon])^(2 + n))^
         m (-1 + \[Epsilon]))), -(((1 - \[Epsilon])^(-1 +
        n) \[Epsilon] (1 - \[Epsilon] + ((1 - \[Epsilon])^(2 + n))^
          m (-(1 - \[Epsilon])^(
             2 + n) + \[Epsilon])))/((-1 + (1 - \[Epsilon])^(
         2 + n)) (1 + (1 - \[Epsilon])^n ((1 - \[Epsilon])^(2 + n))^
          m (-1 + \[Epsilon])))), ((-1 + ((1 - \[Epsilon])^(1 + n))^(
        1 + m)) (1 - \[Epsilon])^n \[Epsilon])/(-1 + (1 - \[Epsilon])^
      n + (1 - \[Epsilon])^
       n ((1 - (1 - \[Epsilon])^(1 + n)) ((1 - \[Epsilon])^(1 + n))^
          m (-1 + \[Epsilon])^2 - \[Epsilon])), ((1 - \[Epsilon])^
      n \[Epsilon] (-1 + ((1 - \[Epsilon])^(1 + n))^
         m ((1 - \[Epsilon])^(
           2 + n) + \[Epsilon])))/(-1 + (1 - \[Epsilon])^
      n + (1 - \[Epsilon])^
       n ((1 - (1 - \[Epsilon])^(1 + n)) ((1 - \[Epsilon])^(1 + n))^
          m (-1 + \[Epsilon])^2 - \[Epsilon]))}, {\[Epsilon], 0, 1},
    PlotStyle -> {RGBColor[1 - n/15, 1 - n/15, 1 - n/15],
      RGBColor[1 - n/15, 1 - n/15, 1 - n/15], RGBColor[1 - m/5, 1, 1],
       RGBColor[1 - m/5, 1, 1], RGBColor[1 - m/5, 1, 1],
      RGBColor[1 - m/5, 1, 1]}, AxesOrigin -> {0, 0},
    AspectRatio -> 1, PlotRange -> {0, 0.5},
    Filling -> {1 -> {{2}, {RGBColor[1 - n/15, 1 - n/15, 1 - n/15]}},
      3 -> {{4}, {RGBColor[1 - m/5, 1, 1], White}},
      6 -> {{5}, {RGBColor[1 - m/5, 1, 1], White}}}], {n, 1, 30}, {m,
    1, 5}];
Show[Plots, AxesLabel -> {\[Epsilon], q},
 AxesStyle -> Directive[Arrowheads[0.02], 16],
 Epilog -> {Text[Style[2, 12], {0.7, 0.4}],
   Text[Style[3, 12], {0.5, 0.225}], Text[Style[4, 12], {0.41, 0.13}],
```

```
    Text[Style[5, 12], {0.37, 0.083}],
   Text[Style[5, 12], {0.33, 0.35}], Text[Style[7, 12], {0.2, 0.236}],
    Text[Style[8, 12], {0.23, 0.3428}],
   Text[Style[7, 12], {0.245, 0.4}]}]
Show[Plots, AxesLabel -> {\[Epsilon], q},
 AxesStyle -> Directive[Arrowheads[0.02], 16],
 Epilog -> {Text[Style[2, 12], {0.7, 0.4}],
   Text[Style[3, 12], {0.5, 0.225}], Text[Style[4, 12], {0.41, 0.13}],
    Text[Style[5, 12], {0.37, 0.083}],
   Text[Style[5, 12], {0.33, 0.35}], Text[Style[7, 12], {0.2, 0.236}],
    Text[Style[8, 12], {0.23, 0.3428}],
   Text[Style[7, 12], {0.245, 0.4}]}]
```

4.1.2 Figure 2.4

```
r = 2
Show[Plot[2/3 - 1/3 (1 + h)^-1, {h, 0, r}, PlotRange -> {1/3, 0.7},
  PlotStyle -> {Red, Thick}, AxesOrigin -> {0, 1/3}],
 Plot[2/3 - 1/3 (1 + h)^-2, {h, 0, 1.5468182768840826},
  PlotRange -> {1/3, 0.7}, AxesOrigin -> {0, 1/3}],
 Plot[2/3 - 1/3 (1 + h)^-2, {h, 1.5468182768840826, r},
  PlotRange -> {1/3, 0.7}, PlotStyle -> {Gray, Dashed},
  AxesOrigin -> {0, 1/3}],
 Plot[2/3 - 1/3 (1 + h)^-3, {h, 0, 0.43965018217331875},
  PlotRange -> {1/3, 0.7}, AxesOrigin -> {0, 1/3}],
 Plot[2/3 - 1/3 (1 + h)^-3, {h, 0.43965018217331875, r},
  PlotRange -> {1/3, 0.7}, PlotStyle -> {Gray, Dashed},
  AxesOrigin -> {0, 1/3}],
 Plot[2/3 - 1/3 (1 + h)^-4, {h, 0, 0.21755508621400235},
  PlotRange -> {1/3, 0.7}, AxesOrigin -> {0, 1/3}],
 Plot[2/3 - 1/3 (1 + h)^-4, {h, 0.21755508621400235, r},
  PlotRange -> {1/3, 0.7}, PlotStyle -> {Gray, Dashed},
  AxesOrigin -> {0, 1/3}],
 Plot[2/3 - 1/3 (1 + h)^-5, {h, 0, 0.13172425293127005},
  PlotRange -> {1/3, 0.7}, AxesOrigin -> {0, 1/3}],
 Plot[2/3 - 1/3 (1 + h)^-5, {h, 0.13172425293127005, r},
  PlotRange -> {1/3, 0.7}, PlotStyle -> {Gray, Dashed},
  AxesOrigin -> {0, 1/3}],
 Plot[{1/6 (2 - 3 h + Sqrt[3] Sqrt[h (4 + 3 h)])}, {h, 0, r},
  PlotStyle -> {Red, Thick}, AxesOrigin -> {0, 1/3}],
 Ticks -> {{{0.13172425293127005,
     Subscript[h, 5]}, {0.21755508621400235,
     Subscript[h, 4]}, {0.43965018217331875,
     Subscript[h, 3]}, {1.5468182768840826, Subscript[h, 2]}, 1,
    0}, {1/3, 2/3}}, AxesLabel -> {h, Subscript[x, 1]},
 AxesStyle -> Directive[Arrowheads[0.02], 16],
 Epilog -> Text[Style[1/3, 11], {-0.02, 0.345}]]
```

4.2 Java Code for Figures 2.6, 3.3 and 3.4

```
import org.eclipse.swt.SWT;
import org.eclipse.swt.graphics.Color;
import org.eclipse.swt.graphics.GC;
import org.eclipse.swt.graphics.Image;
import org.eclipse.swt.graphics.LineAttributes;
import org.eclipse.swt.layout.GridLayout;
import org.eclipse.swt.layout.GridData;
import org.eclipse.swt.widgets.Button;
import org.eclipse.swt.widgets.Canvas;
import org.eclipse.swt.widgets.Display;
import org.eclipse.swt.widgets.Event;
import org.eclipse.swt.widgets.Label;
import org.eclipse.swt.widgets.Listener;
import org.eclipse.swt.widgets.Shell;
import org.eclipse.swt.*;
import org.eclipse.swt.widgets.*;
import org.eclipse.swt.awt.SWT_AWT;
import org.eclipse.swt.events.*;
import org.eclipse.swt.events.*;
public class dreieck {
private static final int TIMER_INTERVAL = 1;
private static final int MAX_PERIOD = 60;
private static final int MAX_WIDTH = 599;
private static final int MAX_HEIGHT =
(int)Math.floor(MAX_WIDTH*Math.sqrt(3)/2)+2;
private static final double PRECISION = 0.02;
private static final int RESOLUTION = 1;
private static Canvas canvas;
public static byte[][] treffer = new byte[MAX_WIDTH+1][MAX_WIDTH+1];

public static double f(double d){
    if (d>0) return d;
    else return 0;
}

public static double auszahlung(int strat, double x, double y, double z){
if (strat==1) return y-z; else
if (strat==2) return z-x; else
if (strat==3) return x-y; else
return 0;
}
```

```
public static void drawconstantdistance(double h,final Display display){
GC gc =new GC(canvas);
int x1 = (int)Math.round(MAX_WIDTH/2-MAX_WIDTH*h/3*Math.sqrt(3)/2);
int y1 = (int)Math.round(MAX_WIDTH*(1-(1+h)/3)*Math.sqrt(3)/2);
int width = (int)Math.round(MAX_WIDTH*2*h/3*Math.sqrt(3)/2);
int height= (int)Math.round(MAX_WIDTH*2*h/3*Math.sqrt(3)/2);

gc.setForeground(display.getSystemColor(SWT.COLOR_GRAY));
gc.drawOval(x1, y1, width, height);
}

public static void drawconstantv(double h,final Display display){
GC gc = new GC(canvas);
gc.setForeground(display.getSystemColor(SWT.COLOR_GRAY));
gc.drawLine((MAX_WIDTH/3),
(int)Math.round((MAX_WIDTH)*Math.sqrt(3)/2),(int)(MAX_WIDTH/3),
(int)Math.round(MAX_WIDTH*(Math.sqrt(3)/6)));
gc.drawLine((int)(MAX_WIDTH/3), (int)Math.round(MAX_WIDTH*(Math.sqrt(3)/6)),
(int)(5*MAX_WIDTH/6),  (int)Math.round(MAX_WIDTH*Math.sqrt(3)/3));
gc.drawLine((int)(5*MAX_WIDTH/6),  (int)Math.round(MAX_WIDTH*Math.sqrt(3)/3),
(MAX_WIDTH/3),(int)Math.round((MAX_WIDTH)*Math.sqrt(3)/2));
}

public static void drawsimplexline(double x1,double y1,double z1,
double x2,double y2,double z2 ,final Display display){
  GC gc = new GC(canvas);
  gc.setForeground(display.getSystemColor(SWT.COLOR_GRAY));
  gc.drawLine((int)Math.round((MAX_WIDTH/2)*(1-x1+y1)),
(int)Math.round(MAX_WIDTH*(1-z1)*Math.sqrt(3)/2),
(int)Math.round((MAX_WIDTH/2)*(1-x2+y2)),
(int)Math.round(MAX_WIDTH*(1-z2)*Math.sqrt(3)/2));
}

public static void rekur(double x,double y,double z,double h,
long counter,long countermax,GC gc){
double nenner = 1+h;
double xneu=0;
double yneu=0;
double zneu=0;
for (int i=0; i< countermax; i++){
if (Math.max(auszahlung(1,x,y,z), Math.max(auszahlung(2,x,y,z),
auszahlung(3,x,y,z)))==auszahlung(1,x,y,z)) xneu=(x+ h)/nenner;
else xneu=x/nenner;
```

```
if (Math.max(auszahlung(1,x,y,z), Math.max(auszahlung(2,x,y,z),
auszahlung(3,x,y,z)))==auszahlung(2,x,y,z)) yneu=(y+ h)/nenner;
else yneu=y/nenner;
if (Math.max(auszahlung(1,x,y,z), Math.max(auszahlung(2,x,y,z),
auszahlung(3,x,y,z)))==auszahlung(3,x,y,z)) zneu=(z+ h)/nenner;
else zneu=z/nenner;
gc.drawLine((int)Math.round((MAX_WIDTH/2)*(1-x+y)),
(int)Math.round(MAX_WIDTH*(1-z)*Math.sqrt(3)/2),
(int)Math.round((MAX_WIDTH/2)*(1-xneu+yneu)),
(int)Math.round(MAX_WIDTH*(1-zneu)*Math.sqrt(3)/2));
if (i == countermax) return;
x=xneu; y=yneu; z=zneu;
}
};

public static void basin(int idxI, int idxJ, double h,int countermax){
double nenner = 1+h;
double[] x = new double[MAX_PERIOD+2];
double[] y = new double[MAX_PERIOD+2];
double[] z = new double[MAX_PERIOD+2];
x[0] = ((MAX_WIDTH/2)-(double)idxI+(double)idxJ/Math.sqrt(3))/MAX_WIDTH;
y[0] = (-(MAX_WIDTH/2)+(double)idxI+(double)idxJ/Math.sqrt(3))/MAX_WIDTH;
z[0] = 1-2*(double)idxJ/(MAX_WIDTH*Math.sqrt(3));
for (long counter = 0; counter <= countermax; counter ++ ) {
for (int j = 3; j <= MAX_PERIOD; j=j+3) {
for (int i = j-3; i < j; i ++ ) {
if (Math.max(auszahlung(1,x[i],y[i],z[i]),
Math.max(auszahlung(2,x[i],y[i],z[i]),
auszahlung(3,x[i],y[i],z[i])))==auszahlung(1,x[i],y[i],z[i]))
x[i+1]=(x[i]+ h)/nenner; else x[i+1]=x[i]/nenner;
if (Math.max(auszahlung(1,x[i],y[i],z[i]),
Math.max(auszahlung(2,x[i],y[i],z[i]),
auszahlung(3,x[i],y[i],z[i])))==auszahlung(2,x[i],y[i],z[i]))
y[i+1]=(y[i]+ h)/nenner; else y[i+1]=y[i]/nenner;
if (Math.max(auszahlung(1,x[i],y[i],z[i]),
Math.max(auszahlung(2,x[i],y[i],z[i]),
auszahlung(3,x[i],y[i],z[i])))==auszahlung(3,x[i],y[i],z[i]))
z[i+1]=(z[i]+ h)/nenner; else z[i+1]=z[i]/nenner;
};
for (int i = 1; i < (int)(j/3); i ++ ) {
int k = j-3*i;
if (Math.abs(x[j]-x[k])+Math.abs(y[j]-y[k])+
Math.abs(z[j]-z[k])< PRECISION){
```

```
treffer[idxI][idxJ]=(byte)(i+1);
return;
}
}
}
x[0]=x[MAX_PERIOD];
y[0]=y[MAX_PERIOD];
z[0]=z[MAX_PERIOD];
}
};

static private void draw(final Display display, double h,double x,
double y,double z,int steps, boolean animate) {
if (animate==true){
// Set up the off-screen GC
Image image = new Image(display, canvas.getBounds());
        GC imageGC = new GC(image);
        //to do: make color handling GUI
        imageGC.setBackground(display.getSystemColor(SWT.COLOR_WHITE));
     imageGC.fillRectangle(0,0,MAX_WIDTH,MAX_HEIGHT);
    for ( int i = 0; i < MAX_WIDTH;  i=i+ RESOLUTION ) {
     for ( int j = 0; j < MAX_WIDTH; j=j+ RESOLUTION ) {
         if (i>=MAX_WIDTH/2-j*Math.sqrt(3)/3 &&
i<=MAX_WIDTH/2+j*Math.sqrt(3)/3 && j<=MAX_WIDTH*Math.sqrt(3)/2){
          treffer[i][j]=0;
          basin(i,j,h,4);
         } else treffer[i][j]= -1;
     }
    }
    for (int i = 1; i <= MAX_WIDTH; i ++ ) {
        for (int j = 1; j <= MAX_WIDTH; j ++ ) {
        if (treffer[i][j]>0){
        imageGC.setForeground(display.getSystemColor(treffer[i][j]+1));
         imageGC.drawPoint(i, j);
        }
        }
}
  contextinfo(display, imageGC);
// Draw the off-screen buffer to the screen
GC canvasGC = new GC(canvas);
canvasGC.drawImage(image, 0, 0);
image.dispose();
imageGC.dispose();
```

```
    }
    else {
     GC canvasGC = new GC(canvas);
        canvasGC.setForeground(display.getSystemColor(SWT.COLOR_BLACK));
        rekur(x,y,z,h,0,steps,canvasGC);
        contextinfo(display, canvasGC);
    }
}

private static void init(final Display display) {
GC canvasGC = new GC(canvas);
    canvasGC.setBackground(display.getSystemColor(SWT.COLOR_WHITE));
canvasGC.fillRectangle(0,0,MAX_WIDTH,MAX_HEIGHT);
contextinfo(display,canvasGC);
}

private static void contextinfo(final Display display, GC imageGC) {
//draw some context info
imageGC.setForeground(display.getSystemColor(SWT.COLOR_GRAY));
imageGC.drawLine((MAX_WIDTH/3),
(int)Math.round((MAX_WIDTH)*Math.sqrt(3)/2),
(MAX_WIDTH/2), (int)Math.round(MAX_WIDTH*Math.sqrt(3)/3));
imageGC.drawLine((int)(MAX_WIDTH/3),
(int)Math.round(MAX_WIDTH*(Math.sqrt(3)/6)),
(MAX_WIDTH/2), (int)Math.round(MAX_WIDTH*Math.sqrt(3)/3));
imageGC.drawLine((int)(5*MAX_WIDTH/6),
(int)Math.round(MAX_WIDTH*Math.sqrt(3)/3), (MAX_WIDTH/2),
(int)Math.round(MAX_WIDTH*Math.sqrt(3)/3));
imageGC.setForeground(display.getSystemColor(SWT.COLOR_BLACK));
imageGC.drawLine((MAX_WIDTH/2), 0, 0, (int)Math.round(MAX_WIDTH*Math.sqrt(3)/2));
   imageGC.drawLine(0, (int)Math.round(MAX_WIDTH*Math.sqrt(3)/2),
MAX_WIDTH,(int)Math.round(MAX_WIDTH*Math.sqrt(3)/2));
   imageGC.drawLine(MAX_WIDTH,(int)Math.round(MAX_WIDTH*Math.sqrt(3)/2),
(MAX_WIDTH/2), 0);
   imageGC.setBackground(display.getSystemColor(1));
imageGC.setForeground(display.getSystemColor(2));
imageGC.drawString("Period:", 2,2);
   for (int i=1; i<= (int)(MAX_PERIOD/3);i++) {
   imageGC.setBackground(display.getSystemColor(i+2));
   imageGC.fillRectangle(5, 14*i, 25, 14*i);
   imageGC.setForeground(display.getSystemColor(1));
   imageGC.drawString(String.valueOf(3*i), 10, 14*i);
   }
```

```
}

public static void main(String[] args) {
final Display display = new Display();
final Shell shell = new Shell(display);
shell.setText("Schere Stein Papier");
GridLayout gridLayout = new GridLayout();
gridLayout.numColumns = 3;
shell.setLayout(gridLayout);
canvas = new Canvas(shell, SWT.COLOR_WHITE);
//set the canvas in the layout
GridData data = new GridData();
data.widthHint = MAX_WIDTH;
    data.heightHint = MAX_HEIGHT;
    data.verticalSpan=50; //we will not use more than 50 rows
canvas.setLayoutData(data);
//add paint listener to canvas
canvas.addPaintListener(new PaintListener() {
  public void paintControl(PaintEvent event) {
    // Draw the background
event.gc.setBackground(shell.getDisplay().getSystemColor(SWT.COLOR_WHITE));
    event.gc.fillRectangle(0,0,MAX_WIDTH,MAX_WIDTH);
  }
});

//now add interface components

Label labelStartH = new Label(shell, SWT.PUSH);
final Text textStartH = new Text(shell, SWT.MULTI|SWT.WRAP);
{
    labelStartH.setText("StartH:");
GridData datatextStartH = new GridData();
datatextStartH.widthHint = 50;
textStartH.setLayoutData(datatextStartH);
textStartH.setText("0.4");
}
Label labelEndH = new Label(shell, SWT.PUSH);
final Text textEndH = new Text(shell, SWT.MULTI|SWT.WRAP);
{
    labelEndH.setText("EndH:");
GridData datatextEndH = new GridData();
datatextEndH.widthHint = 50;
textEndH.setLayoutData(datatextEndH);
```

```
textEndH.setText("0.4");
}

Label labelNumSteps = new Label(shell, SWT.PUSH);
final Text textNumSteps = new Text(shell, SWT.MULTI|SWT.WRAP);
{
    labelNumSteps.setText("NumSteps:");
GridData datatextNumSteps = new GridData();
datatextNumSteps.widthHint = 50;
textNumSteps.setLayoutData(datatextNumSteps);
textNumSteps.setText("1");
}

Label labelsteps = new Label(shell, SWT.PUSH);
final Text textSteps = new Text(shell, SWT.MULTI|SWT.WRAP);
{
labelsteps.setText("steps");
//use grid data for formatting:
GridData datatextSteps = new GridData();
datatextSteps.widthHint = 50;
textSteps.setLayoutData(datatextSteps);
textSteps.setText("100");
}
Button animateButton = new Button(shell, SWT.PUSH);
animateButton.setText("animate");
animateButton.addSelectionListener(new SelectionAdapter() {
    public void widgetSelected(SelectionEvent e) {

     double startH = Double.parseDouble(textStartH.getText());
     double endH = Double.parseDouble(textEndH.getText());
     double numSteps = Double.parseDouble(textNumSteps.getText());
     for(int i=1;i<=numSteps;i++) {
     //double s = 1-(double)1/Math.pow(1.2,i);
     double s = 1-(double)i/(numSteps);
     double h= endH+ s*s*(startH-endH);
     draw(display,h,0.3,0.3,0.4,0,true);

     double xx=((2-3*h+Math.sqrt(3*h)*Math.sqrt(3*h+4))/6+h)/(1+h);
     double yy=1/3.0/(1+h);
     double zz=(2+3*h-Math.sqrt(3*h)*Math.sqrt(3*h+4))/6/(1+h);

     drawsimplexline(xx,yy,zz,zz,xx,yy,display);
     drawsimplexline(zz,xx,yy,yy,zz,xx,display);
```

```
     drawsimplexline(yy,zz,xx,xx,yy,zz,display);
     xx=(1+2*h)/(3*(1+h));
     yy=1/3.0;
     zz=1/(3*(1+h));

     drawsimplexline(xx,yy,zz,zz,xx,yy,display);
     drawsimplexline(zz,xx,yy,yy,zz,xx,display);
     drawsimplexline(yy,zz,xx,xx,yy,zz,display);

     try{
     // good night...
     Thread.sleep(TIMER_INTERVAL);
     }
     catch(InterruptedException ie){
     //we don't handle this
     }
     }
    }
});

Button initButton = new Button(shell, SWT.PUSH);
initButton.setText("init");
initButton.addSelectionListener(new SelectionAdapter() {
    public void widgetSelected(SelectionEvent e) {
     init(display);
    }
});
    canvas.addMouseListener(new MouseListener() {
      public void mouseDoubleClick(MouseEvent me) {
     double endH = Double.parseDouble(textEndH.getText());
     //  double numSteps = Double.parseDouble(textNumSteps.getText());
     int idxI = me.x;
     int idxJ = me.y;
     double x = (MAX_WIDTH/2-(double)idxI+(double)idxJ/Math.sqrt(3))/MAX_WIDTH;
     double y = (-MAX_WIDTH/2+(double)idxI+(double)idxJ/Math.sqrt(3))/MAX_WIDTH;
     double z = 1-2*(double)idxJ/(MAX_WIDTH*Math.sqrt(3));
     int steps=Integer.parseInt(textSteps.getText());
       draw(display, endH,x,y,z,steps,false);
      }
@Override
public void mouseDown(MouseEvent e) {
// TODO Auto-generated method stub
```

```
}
@Override
public void mouseUp(MouseEvent e) {
// TODO Auto-generated method stub
}
 });
shell.pack();
shell.open();

while (!shell.isDisposed()) {
  if (!display.readAndDispatch()) {
    display.sleep();
  }
}
display.dispose();
}
}
```

List of Figures

References

[1] R. Dawkins, *The Selfish Gene*, Oxford University Press, USA, 2006.

[2] J. Hofbauer, *From Nash and Brown to Maynard Smith: Equilibria, Dynamics and ESS*, Selection **1** (2000), 81–88.

[3] J. Hofbauer and K. Sigmund, *Evolutionary games and population dynamics*, Cambridge University Press, 1998.

[4] L. Gardini, F. Tramontana, V. Avrutin, M. Schanz, *Border-Collision Bifurcations in 1D Piecewise-Linear Maps and Leonov's Approach*, International Journal of Bifurcation and Chaos **20** (2010), no. 20, 3085–3104.

[5] N.N. Leonov, *Map of the Line onto Itself*, Radiofisika **2(6)** (1959), 942–956.

[6] H.E. Nusse and J.A. Yorke, *Border-collision bifurcations including period two to period threefor piecewise smooth maps*, Physica D: Nonlinear Phenomena **57** (1992), no. 1-2, 39–57.

[7] J. Maynard Smith and G.A. Parker, *The logic of asymmetric contests*, Animal Behaviour **24** (1976), 159–175.

Curriculum Vitae

Personal Data

Name:	Peter Bednarik
Date of Birth:	11th February, 1984
Birth Location:	Bratislava, Slovakia
Nationality:	Austria

Education

2002:	Matura (A-Levels) at Theresianische Akademie Wien
2002 - 2006:	Electrical Engineering at Vienna University of Technology
2004 - 2005:	Jazz guitar at Vienna Music Institute
2006 - 2011:	Mathematics at University of Vienna
2009/10:	Study Abroad at University of Leeds, UK

Selected Work

Summer 2000:	Work Experience Siemens AG
2002 - 2003:	Shell Austria AG, Assistant in Corporate Quality Management
2004 - 2006:	Fast Forward Studios GmbH, Sound Engineer
2010 - 2011:	Assistant for Mathematics Practical at University of Natural Resources and Life Sciences, Vienna